

Orion Outlying Clouds

Juan M. Alcalá, Elvira Covino and Silvio Leccia

INAF- Osservatorio Astronomico di Capodimonte,
Via Moiariello 16, 80131, Naples, Italy

Abstract. In this chapter we review the properties of the Orion outlying clouds at $b < -21^\circ$. These clouds are located far off the Orion giant molecular cloud complex and are in most cases small cometary-shaped clouds, with their head pointing back towards the main Orion clouds. A wealth of data indicate that star formation is ongoing in many of these clouds. The star formation in these regions might have been triggered due to the strong impact of the massive stars in the Orion OB association. Some of the clouds discussed here may be part of the Orion-Eridanus bubble. An overview on each individual cloud is given. A synthesis of the Pre-Main Sequence stars discovered in these clouds is presented. We also discuss the millimeter and centimeter data and present a review of the outflows and Herbig-Haro objects so far discovered in these clouds.

1. Introduction

The Orion Outlying Clouds are typically small clouds located in the outskirts of the Orion molecular cloud complex. Most of the known clouds of this kind are located to the west of the Orion OB association. They often appear as small cometary clouds, which point back towards the Orion OB association and in which star formation might have been triggered due to the strong impact of the massive stars in the Orion OB association. The illumination of dense clumps in molecular clouds by OB stars could be responsible for their collapse and subsequent star formation. The UV radiation from the OB stars may sweep the molecular cloud material into a cometary shape with a dense core located at the head of the cometary clouds. Bright Rimmed Clouds (BRCs) associated with HII regions are examples where the UV flux of a nearby OB star ionizes the external layers of the cloud and causes the BRC to collapse. The shape of a BRC (curved or cometary-like) is governed by the ionization fronts from the OB stars that, compressing the head of the BRC, enhance the density of the outer layers of the cloud. This process may lead to sequential star formation. Sugitani, Fukui & Ogura (1991) and Sugitani & Ogura (1994) catalogue 89 BRCs associated with IRAS point sources in both the northern and southern hemispheres, some of which are also associated with Herbig-Haro objects and molecular outflows. These BRCs are sites in which triggered star formation might have taken place.

In this chapter we discuss the outlying clouds in Orion at $b < -21^\circ$, focusing mainly on the four best studied cases, namely L 1615/L 1616, L 1634, the IC 2118 region and L 1642. However, few aspects of other high-galactic latitude clouds are also mentioned. Some of these clouds may be inside the so called Orion-Eridanus bubble, a cavity of the interstellar medium towards Orion which is filled with hot ionized gas surrounded by an expanding shell of neutral hydrogen. For a detailed description of

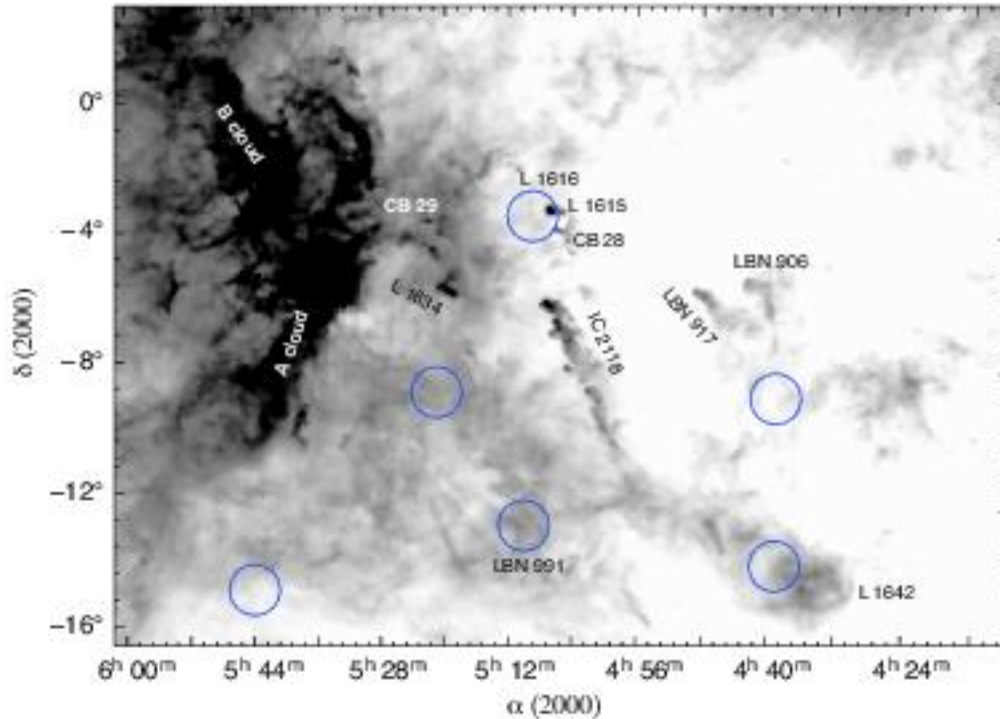


Figure 1. Map of the $100\ \mu\text{m}$ IRAS dust emission of the Orion OB association. The main Orion molecular clouds A and B are indicated. The Orion outlying clouds discussed in this chapter are labelled. The big circles represent the ROSAT X-ray clumps that satisfy the Sterzik et al. (1995) criteria.

the Orion-Eridanus bubble we refer the reader to Brown, Hartmann & Burton (1995). We use the $100\ \mu\text{m}$ IRAS map in order to identify the Orion outlying clouds discussed here and refer to Figure 1 for their spatial location and to Table 1 for their approximate coordinates, in order of decreasing Galactic latitude.

In addition to the Orion outlying clouds we also discuss a few topics of the four small bright-rimmed clouds and cometary globules No. 27, 35, 40 and 41 by Ogura & Sugitani (1998), which are located in the vicinity of the O7 V star σ Ori.

The PMS objects in each of the outlying clouds and globules are also discussed. A number of $H\alpha$ -emission stars are found on the clouds, but other are scattered around them. Their coordinates, designations and other informations are synthesized and reported in a table (Table 9). For many of these stars a proper motion determination is provided in the catalogue by Ducourant et al. (2005). The objects in the Orion OB1a association are not discussed here, but they are treated in other chapters of this book. While some $H\alpha$ -emission stars in the outer regions of Orion were discovered in the objective-prism survey by Stephenson (1986), many others were revealed in the Kiso $H\alpha$ survey (Wiramihardja et al. 1991; Nakano, Wiramihardja, & Kogure 1995). Other weak $H\alpha$ -emission stars in these regions were identified as optical counterparts of the ROSAT All-Sky Survey sources in spectroscopic follow-ups (e.g. Alcalá et al. 1996, 2000).

Table 1. Orion outlying clouds discussed in this chapter

Cloud	$\alpha(2000)$ h m s	$\delta(2000)$ ° ' "	l (°)	b (°)	other IDs	refs.
CB 29	05:22:12	-03:41:34	205.8	-21.5		1
L 1634	05:19:49	-05:52:05	207.6	-23.0	MBM 110	2, 3
L 1616 [†]	05:07:00	-03:21:06	203.5	-24.7		2
L 1615 [†]	05:05:30	-03:26:00	203.4	-25.1		2
CB 28	05:06:20	-03:56:22	204.0	-25.1	LBN 923	1, 2
IC 2118	05:03:55	-08:23:59	208.1	-27.7		4
LBN 991 [†]	05:11:00	-12:24:00	213.1	-27.8		2
LBN 917	04:47:42	-05:55:00	203.5	-30.1	DIR 203-32	2, 5
LBN 906	04:41:00	-05:24:00	202.1	-31.4		2
L 1642 [†]	04:35:03	-14:13:57	210.9	-36.6	LBN 981, MBM 20	2, 3

[†] coinciding with an X-ray clump (see Sect. 1).

References: 1: Clemens & Barvainis (1988); 2: Lynds (1962); 3: Magnani, Blitz & Mundy (1985); 4: Dreyer (1908); *Index Catalog*; 5: Reach, Wall & Odegard (1998)

The complete sky coverage of the ROSAT All-Sky Survey permits an unbiased analysis of the spatial distribution of X-ray active stars, though it is flux limited. Sterzik et al. (1995) established a criterion for selecting young star candidates from ROSAT All-Sky Survey sources based on X-ray hardness ratios and the ratio of X-ray to optical flux, and used this to trace their spatial distribution in a $\sim 700 \text{ deg}^2$ field around the Orion molecular clouds. The surface density distribution reproduces the major clusters associated with the OB sub-group associations (OB1a, OB1b, OB1c, and λ -Ori), and the spatial extent of the clusters is consistent with dispersal times between 2 and 10 Myrs, e.g. the respective ages of the stellar components in those regions. The same analysis revealed several overdensities of X-ray sources with high probability of being low-mass PMS stars (Sterzik et al. 1995; Walter et al. 2000). Several of these X-ray clumps are located far from the main Orion molecular clouds and some of them are coincident with or very close in position to the Orion outlying clouds, in particular L 1615/L 1616, LBN 991 and L 1642. Some of these clumps are indicated with circles in the $100 \mu\text{m}$ IRAS map in Figure 1. It is interesting to note that L 1634 and IC 2118 were not revealed as X-ray enhancements in the analysis by Sterzik et al. (1995) (see Figure 1). This may be an indication that the X-ray emitting young stellar population in these regions is less conspicuous, or that the objects are much younger, and/or more embedded, than in other clouds revealed as X-ray clumps like L 1616.

The chapter is structured as follows: an overview of the L 1634, L 1616/L 1615, IC 2118 and L 1642 clouds and their young populations are presented in Sections 2, 3, 4 and 5 respectively, while other small clouds are discussed in Section 6. The four small clouds around σ Ori are then discussed in Section 7, while a synthesis of the distances of the outlying clouds is presented in Section 8. Finally, a summary is presented in Section 9.

2. L 1634

L 1634 (Lynds 1962) is a small, isolated dark cloud located some 3 degrees to the west of the Orion A cloud (cf. Figure 1). A color image of the cloud is shown in Figure 2. The Red Nebulous Object No. 40 (RNO-40 following the nomenclature by Cohen 1980) or SFO-16 (following Sugitani, Fukui & Ogura 1991) is a small nebulous object in L 1634. This nebulous object was catalogued as a star with a tailed nebula by Gyul'budaghian & Magakian (1977, their object No. 38) and coincides with object PP 27 by Parsamian & Petrosian (1979). The object is seen in the zoomed area in Figure 2. The L 1634 cloud also coincides with the MBM 110 cloud (Magnani, Blitz & Mundy 1985) and with the CO emission peak No. 14 reported by Maddalena et al (1986). The Lynds bright nebulae (Lynds 1965) LBN 956, LBN 957 and LBN 964 are nearby L 1634, while LBN 960 is located on the cloud (see Figure 3). The coordinates of these bright nebulae are listed in Table 2.

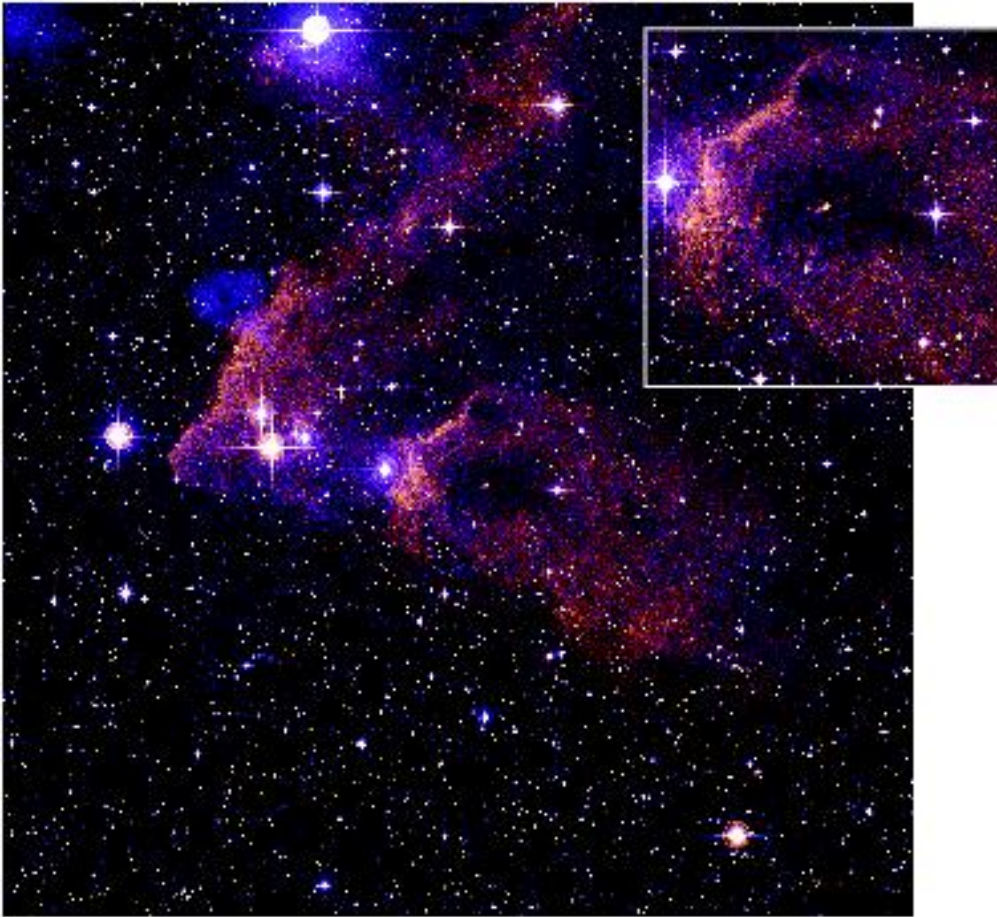


Figure 2. The left panel is a color image of the L 1634 cometary cloud. The image was produced by the authors by combining three Digitized Sky Survey (DSS) images. It covers a field of $60' \times 60'$. North is up and East to the left. The central region is zoomed in the right panel, which covers an area of $25' \times 25'$.

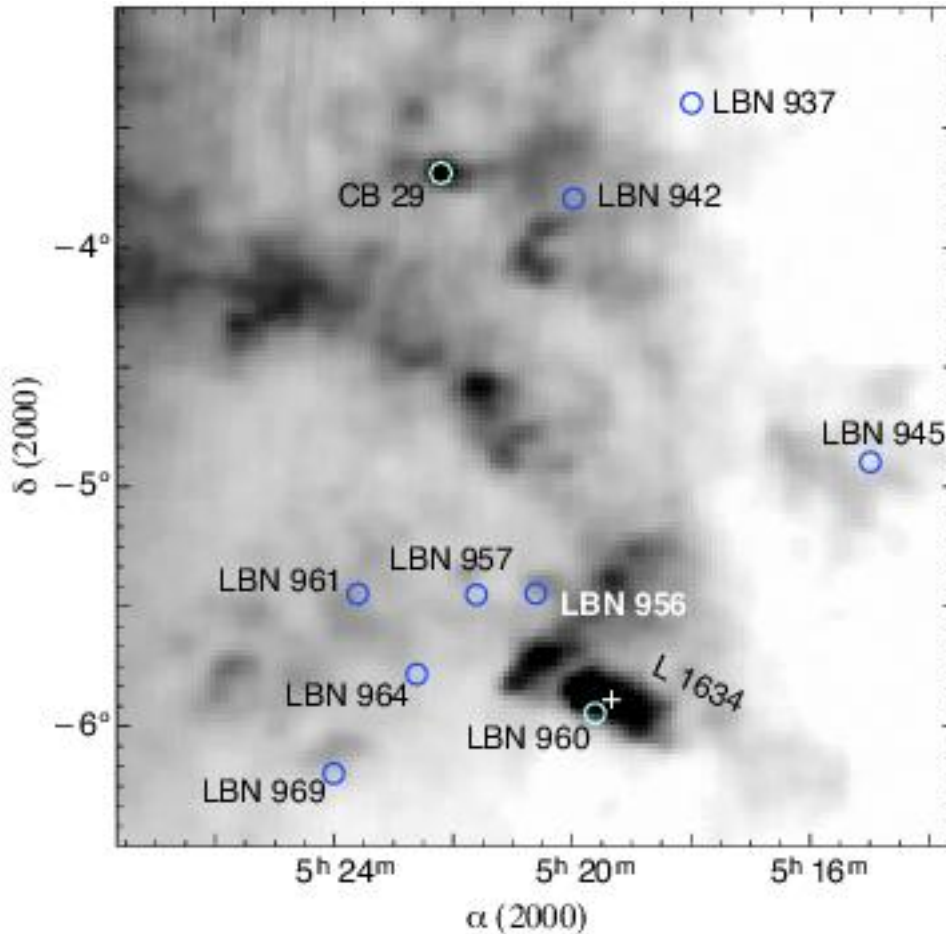


Figure 3. Map of the IRAS $100\ \mu\text{m}$ dust emission of the region in the L 1634 cometary cloud. The position of the source IRAS 05173–0555, which drives the spectacular outflow in L 1634, is indicated by the white *plus* symbol. The position of CB 29 as reported in Table 1, as well as of other Lynds bright nebulae, whose coordinates are listed in Table 2, are indicated with circles.

L 1634 was first studied in the CO ($J=1 \rightarrow 0$ transition) by Torrelles et al. (1983). The cloud has been proposed to be either a remnant of the molecular material from which the nearby Orion OB1 association formed or a cloud pushed to its present location by the pressure associated with energetic phenomena accompanying the evolution of the OB association (Maddalena et al 1986). L 1634, which borders Barnard’s loop, is classified as a type-A bright-rimmed cloud rather than as a cometary cloud, because it has a broad ionization front with no tail (Sugitani, Fukui & Ogura 1991).

The infrared source IRAS 05173–0555 is located in this cloud. Cohen (1980) described the object as a purely nebulous, elongated, very red source typical of Herbig-Haro (HH) objects, with an emission line spectrum including $H\alpha$, $H\beta$, $H\gamma$, [N II], [S II], [O I], [N I], [O III], and He I. Indeed, the L 1634 cloud is much better known because its core hosts two spectacular outflows and the Herbig-Haro objects HH 240/241. The powerful outflow is driven by the aforementioned IRAS source (Davis et al. 1997) and

most of the research done so far in this cloud has been focused on the investigation of the outflows.

2.1. L 1634: PMS Stars

A number of $H\alpha$ emission-line stars are found on/or very close to the cloud. Many of these stars are located east of the cloud, which may be taken as an indication that they are a possible result of induced star formation. There are three $H\alpha$ emission-line stars detected in the survey by Stephenson (1986), namely StHA 37, StHA 38 and StHA 39. The star StHA 37 coincides with HBC 83 of the Herbig & Bell (1988) catalogue¹, which can be also identified with the IRAS source IRAS 05178–0548 and the $H\alpha$ -emission star Kiso A-0975 52. StHA 38 coincides with V 534 Ori, while StHA 39 was also detected in X-rays in the ROSAT All-Sky Survey (Alcalá et al. 1996). Both StHA 38 and StHA 39 can be classified as T Tauri stars based on follow-up spectroscopic observations (Downes & Keyes 1988; Lee & Chen 2007). There are thus at least three on-cloud T Tauri stars in L 1634, whose coordinates are reported in Table 9. Two objects classified as T Tauri stars based on follow-ups of the ROSAT All-Sky Survey X-ray sources (Alcalá et al. 1996, 2000) are scattered in the field of L 1634 and CB 29 and are also indicated as T Tauri stars in Table 9.

Table 2. Lynds bright nebulae in the field of L 1634 and CB 29.

Cloud	RA (2000) h m s	DEC(2000) ° ' "	l (°)	b (°)
LBN 960	05:19:37	−05:56:51	207.66	−23.11
LBN 956	05:20:37	−05:26:51	207.29	−22.66
LBN 957	05:21:37	−05:27:14	207.42	−22.44
LBN 964	05:22:37	−05:47:03	207.86	−22.37
LBN 961	05:23:36	−05:27:04	207.66	−22.00
LBN 942	05:19:59	−03:47:57	205.63	−22.04
LBN 937	05:18:00	−03:24:00	205.00	−22.29
LBN 945	05:15:00	−04:53:51	206.06	−23.65
LBN 969	05:24:01	−06:12:01	208.43	−22.25

In addition to the previously known PMS stars, we have selected other $H\alpha$ -emission stars within a radius of about 1.3 degrees from the two cloud centers. This radius was derived considering that 10 Myr old stars at a distance of 450 pc drifting with a velocity dispersion of 1 km/s spread-out within a radius of about 10 pc from the clouds center. Using in addition the 2MASS data and the criteria by Lee et al. (2005) we selected 6 $H\alpha$ -emission stars that have a high probability of being T Tauri stars based on their near-IR colors. Two of these stars coincide with previously known T Tauri stars (namely, StHA 37 and StHA 38). We report the other 4 stars in Table 9 as T Tauri star candidates in L 1634.

¹In the Herbig & Bell (1988) catalogue, the entry HBC 83, corresponding to StHA 37, is erroneously associated with the star V 534 Ori (which actually coincides with StHA 38).

2.2. L 1634: Infrared, Centimeter and Millimeter Sources

The two most interesting IR sources in the L 1634 cloud are IRAS 05173–0555 and LDN 1634 7 (Hodapp & Ladd 1995; Davis et al. 1997). Their coordinates are given in Table 9. Reipurth et al. (1993) measured the source flux at 1300 μm and confirmed that it is a deeply embedded source. They also detected cool dust emission toward the IRAS source. IRAS 05173–0555 has a bolometric luminosity of $17 L_{\odot}$ (Reipurth et al. 1993; Hodapp & Ladd 1995) and may be a transition object between the Class-0 and Class-I phases (Reipurth et al. 1993; Beltrán et al. 2002).

Beltrán et al. (2002) reported observations of the centimeter, millimeter, and sub-millimeter continuum emission toward the core of L 1634. They detected five radio continuum sources at centimeter and millimeter wavelengths. One of these (VLA 3) coincides with IRAS 05173–0555. The other four are listed in Table 9 as YSOs candidates. Beltrán et al. (2002) found that the sub-millimeter dust emission around IRAS 05173–0555 is resolved and shows two components, a centrally peaked source plus a considerably extended envelope, while the emission around LDN 1634 7 appears unresolved. They also found that the dust properties around the two IR sources are similar. Based on a power-law model of the radial intensity profiles of the extended emission, they constrain the density distribution around IRAS 05173–0555 and find that the best fit is consistent with the predictions of the inside-out protostellar collapse model. They derive an infall-mass rate of $(2.6\text{--}8.0)\times 10^{-5} M_{\odot} \text{ yr}^{-1}$ for the free-falling inner region of the envelope and conclude that the sub-millimeter luminosity, the total circumstellar mass derived, and the infall-rate estimate are consistent with IRAS 05173–0555 being a Class-0 object.

In a study of bright-rimmed clouds that includes L 1634, De Vries et al. (2002) reported the results of a millimeter and sub-millimeter molecular line survey. They found that the appearance of the millimeter CO and HCO^{+} emission is dominated by the morphology of the shock front in the bright-rimmed clouds. The HCO^{+} ($J = 1\text{--}0$) emission tends to trace the swept-up gas ridge and overdense regions, which may be induced to collapse as a result of sequential star formation. In the case of L 1634, the millimeter and sub-millimeter HCO^{+} observations by De Vries et al. (2002) show some evidence of infall asymmetry.

In addition, there are four IRAS sources in the neighborhood of the small cloud CB 29. These are IRAS 05194–0343, IRAS 05194–0346, IRAS 05201–0341 and IRAS 05190–0348.

2.3. L 1634: Outflows and Herbig-Haro Objects

The core of L 1634 is probably much better known as the site of the spectacular bipolar outflow and the Herbig-Haro objects HH 240/241 (in the catalog of Reipurth 2000). The object was originally named RNO 40 by Cohen (1980). HH 240/241 in the infrared H_2 lines are revealed as a powerful bipolar flow (Hodapp & Ladd 1995; Davis et al. 1997) extending in the East-West direction from both sides of the infrared source IRAS 05173–0555 (cf. Figure 4). This source is indicated to be driving the outflow by the CO ($J=3\text{--}2$) spectra obtained by Davis et al. (1997) and has a steeply rising spectral energy distribution from 12 to 100 μm (Cohen, Harvey & Schwartz 1985). The L 1634 powerful outflow has a total length of about $6'$, corresponding to a projected length of about 0.8 pc at a distance of 450 pc. The bright HH knots A, B, C and D identified by Davis et al. (1997) along the outflow are shown in Figure 4, and their coordinates are

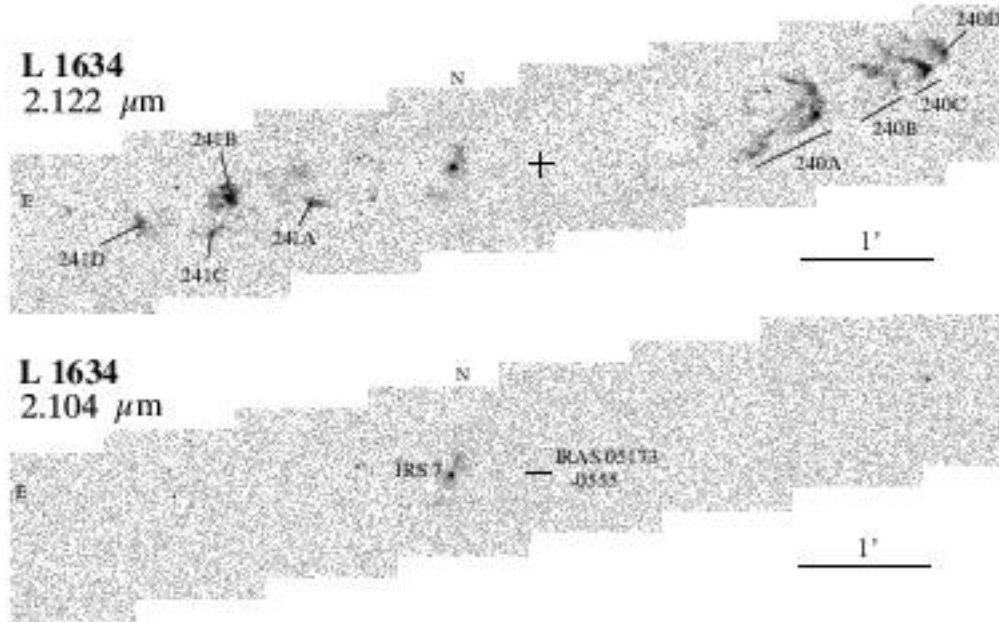


Figure 4. Narrow-band images of the L 1634 outflow at $2.122 \mu\text{m}$ (H_2 + continuum) and $2.104 \mu\text{m}$ (continuum). The position of the driving source of the outflow IRAS 05173–0555 is marked with a cross. The IR source LDN 1634 7, which might drive the other outflow in L 1634, is also indicated as IRS 7. Adapted from Davis et al. (1997).

Table 3. Herbig-Haro Objects in L 1634[‡].

Cloud	RA (2000) h m s	DEC(2000) ° ' "	cloud	driving source
HH 240A [†]	05:19:40.45	−05:51:42.3	L 1634	IRAS 05173–0555
HH 240B	05:19:38.66	−05:51:23.2	L 1634	IRAS 05173–0555
HH 240C	05:19:37.06	−05:51:21.0	L 1634	IRAS 05173–0555
HH 240D	05:19:36.56	−05:51:14.0	L 1634	IRAS 05173–0555
HH 241A	05:19:57.03	−05:52:24.5	L 1634	IRAS 05173–0555
HH 241B	05:19:58.24	−05:52:20.6	L 1634	IRAS 05173–0555
HH 241C	05:19:58.83	−05:52:35.6	L 1634	IRAS 05173–0555
HH 241D	05:20:01.13	−05:52:33.8	L 1634	IRAS 05173–0555

[‡]: data adapted from Davis et al. (1997); Hodapp & Ladd (1995)

[†]: this knot coincides with Kiso A-0975 48

reported in Table 3. The object catalogued as the emission-line star Kiso A-0975 48 coincides with the Herbig-Haro object HH 240A.

Nisini et al. (2002) performed an extensive 1-2.5 μm spectroscopic survey of the bright HH knots (A, B, C and D) identified by Davis et al. (1997) along the two Herbig-Haro chains HH240-HH241, i.e. the blue-shifted (HH 240) and red-shifted (HH 241) lobes of the bipolar outflow in L 1634, respectively (see Figure 4). They found that the spectra are characterized by prominent emission of both [Fe II] and H₂ transitions. The intensity of the [Fe II] lines decreases when moving away from the driving source. In addition to the [Fe II] and H₂ lines, emission from other species such as [C I], [S II], [N I], as well as recombination lines from the Paschen series are detected. These lines are used by Nisini et al. (2002) as a reference to infer the gas-phase iron abundance in the observed HH objects.

In a detailed near-IR spectroscopic study O’Connell et al. (2004) found that, while the CO emission of the bow shocks in the L 1634 protostellar outflow originates from cloud gas directly set in motion, the H₂ emission is generated from shocks sweeping through an outflow. Considering optical data, O’Connell et al. reached a similar conclusion of a global outflow model involving episodic, slow-precessing, twin jets.

The IR source LDN 1634 7, named IRS 7 by Hodapp & Ladd (1995) and located 50” East of IRAS 05173–0555 (see Figure 4 and Hodapp & Ladd 1995; Davis et al. 1997), may be associated with a second independent outflow, which extends towards northwest and southeast (see Figure 4). The jet associated with LDN 1634 7 seems to have only two knotty bow shocks (knots 9 and 4 by Hodapp & Ladd 1995). Seale & Looney (2008) reported Spitzer data of LDN 1634 7 and IRAS 05173–0555.

3. L1616 and L 1615

The clouds L 1616 and L 1615 (Lynds 1962) form a cometary cloud located about 6 degrees west of the Orion giant molecular clouds (see Figure 1). The pair of clouds subtends about 40’ (5.2 pc at a distance of 450 pc) roughly in the east-west direction. The head (L 1616), pointing toward east, in the general direction of the Orion OB associations (see Figures 1 and 6), harbors the NGC 1788 reflection nebula, which is illuminated mainly by the B9V-type star HD 293815. A three-color image of L 1616 and L 1615 is provided in Figure 5. L 1616 and L 1615 are apparently shaped by the winds and radiation coming from the massive, hot stars of the OB association.

Ramesh (1995) performed a CO survey in the head of the L 1616 cometary cloud and Stanke et al. (2002) reported on mid-infrared (MIR) and millimeter observations of the L 1616 region, which revealed five MIR sources, associated with very young stellar objects, and four millimeter sources, the brightest of which may be a Class-0 protostar that drives a powerful jet. The data of Stanke et al. (2002) revealed traces of ongoing star formation in the cloud and in the NGC 1788 reflection nebula in the head of the cometary cloud. The location of the protostar discovered by Stanke et al. (2002) with respect to other young stars in L 1616 and towards the OB association suggests an age sequence due to a wave of star formation propagating through the cloud and triggered by the impact of the nearby OB association.

A conspicuous X-ray clump was detected in L 1616 and L 1615 (Sterzik et al. 1995) which suggested the existence of a small star forming region. Prior to the RASS, the only known young star in the region was the T Tauri star LkH α 333. This triggered subsequent X-ray observations using the High-Resolution Imager onboard ROSAT; Al-

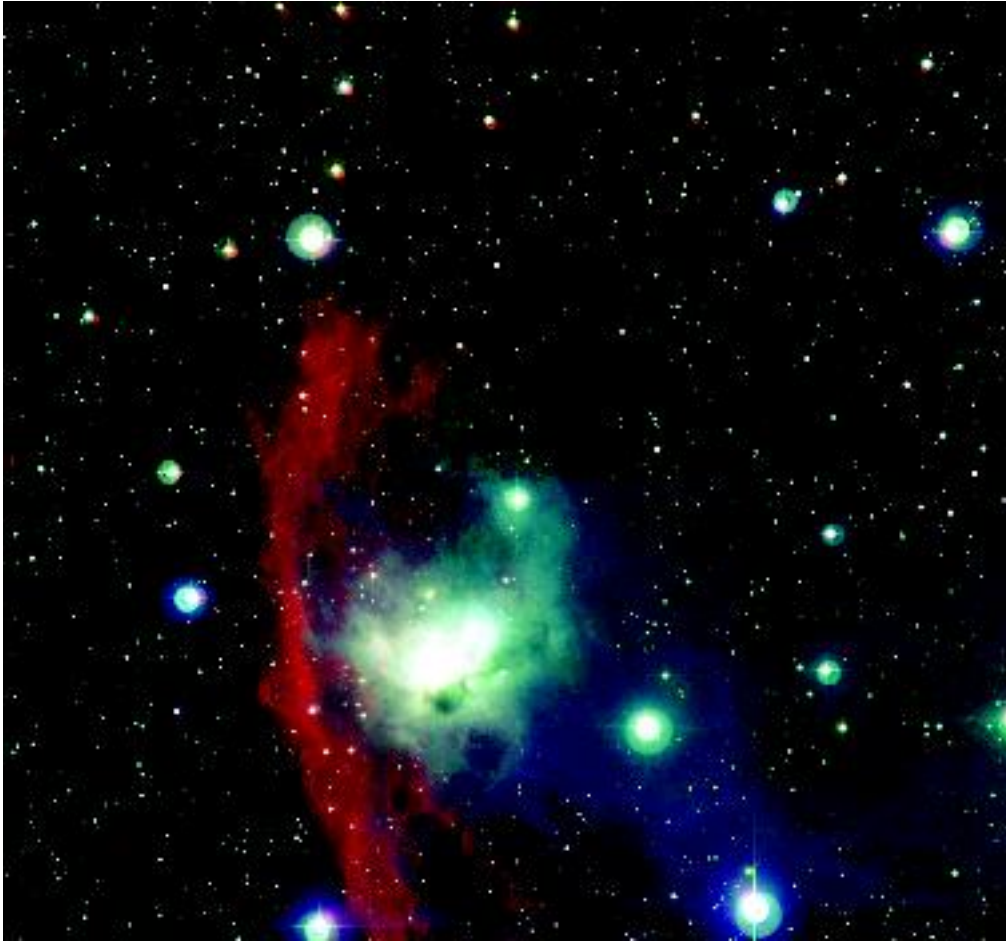


Figure 5. Three-color mosaic of L 1616 and L 1615 produced by the authors by combining images taken in the R , I , and $H\alpha$ filters. The images were acquired using the Wide Field Imager on the ESO-MPI 2.2m telescope at La Silla. The assigned colors are blue, yellow and red for the R , I , and $H\alpha$ bands respectively. The image covers a field of about $30' \times 30'$. North is up and East to the left. $H\alpha$ nebular emission produced by the impact of the hot stars in the OB association to the north-east appears as an almost vertical "red" lane. The NGC 1788 reflection nebula is clearly seen to the right of the $H\alpha$ lane.

calá et al. (2004) performed a multi-wavelength study of the L 1616 region, from X-ray to near-IR wavelengths. They found more than 20 new low-mass PMS stars distributed mainly to the east of L 1616 in about a 1-square-degree field. They also found that the X-ray properties of the PMS stars in L1616 are quite similar to those of PMS stars detected in the Orion Nebula Cluster. They derived the stellar parameters for 32 stars in the region and, based on the level of X-ray emission, lithium content and kinematics, they confirmed the PMS nature of these stars, as well as their association with L 1616. By comparing the position of these stars in the HR diagram with PMS evolutionary

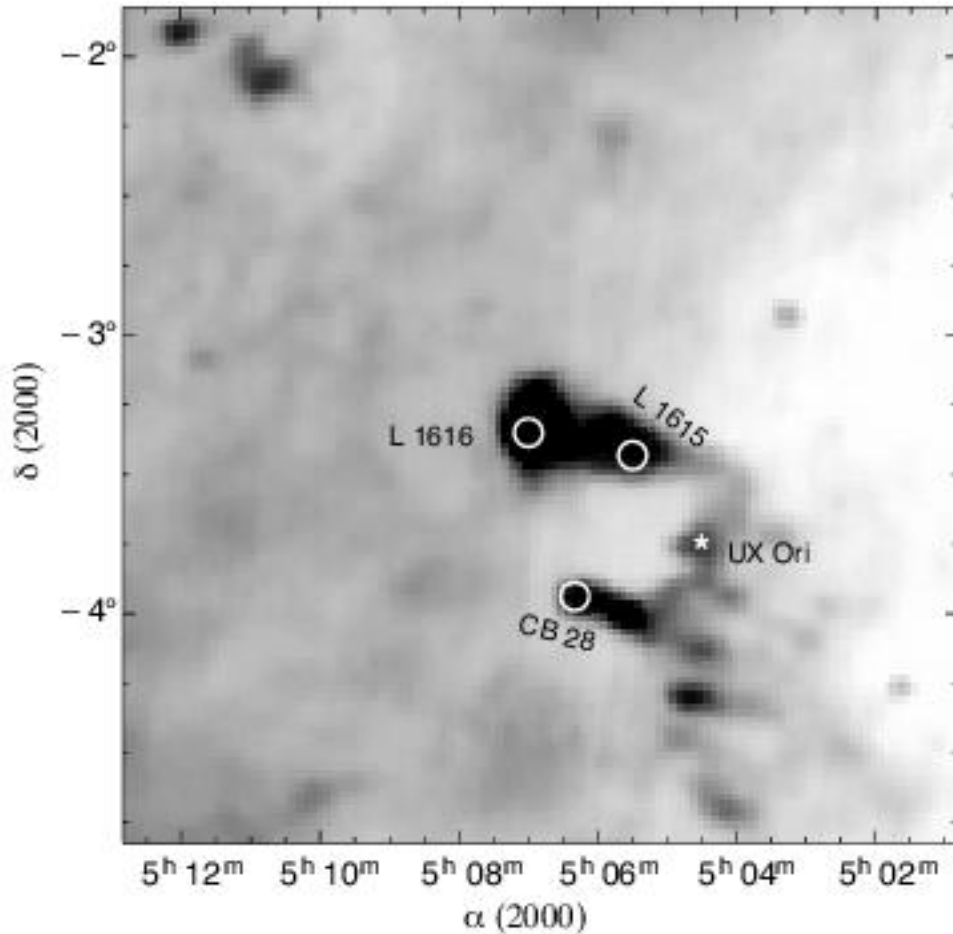


Figure 6. Map of the $100\ \mu\text{m}$ IRAS dust emission of the region around the L 1616 cometary cloud. The positions of L 1615, L 1616, and CB 28 as reported in Table 1 are indicated with circles. The asterisk represents the star UX Ori.

tracks, they inferred an age of about 1-2 Myr with a dispersion of about 1 Myr. The small age dispersion can be explained in terms of efficient and very rapid star formation.

Based on CO observations, Ramesh (1995) found an excess velocity of about $1.5\ \text{km s}^{-1}$ above the virial equilibrium velocity of the cloud, which implies that the virial mass of the cloud is about five times larger than the observed value. Ramesh (1995) hence concluded that the energy input due to the stars in the cluster is fragmenting the cloud and, given its size of about 2 pc, the excess motions of the gas above the virial equilibrium suggest that the fragmentation process may have lasted for the past 1-2 Myr. The latter figure is consistent with the age derived by Alcalá et al. (2004) for the L 1616 stars.

The most recent census of the PMS population of L 1616/L 1615 is presented in Gandolfi et al. (2008). They characterized the young population of the region and concluded that L 1616/L 1615 can be considered as a small cluster according to the

criterion by Lada & Lada (2003). Gandolfi et al. (2008) also derived the Initial Mass Function of the region, concluding that it is consistent with that of the field.

Another important issue is the high star formation efficiency in L 1616. From his CO observations, Ramesh (1995) determined a total mass of $180 M_{\odot}$ for the cloud. The total mass in PMS stars in L 1616 is at least $30 M_{\odot}$. Therefore, the star formation efficiency (mass in stars to total mass fraction) is about 14% (Ramesh 1995; Alcalá et al. 2004), which is significantly high when compared with the average value of a few percent ($<3\%$), derived for other nearby star forming regions. The recent investigation by Gandolfi et al. (2008) indicates a lower value (about 8%) but it is still high in comparison with the canonical values.

Given the spatial distribution of the PMS stars relative to the head of the cloud (see Figure 7), as well as its cometary shape and high star formation efficiency, the star formation in L 1615/L 1616 may have occurred due to a single triggering event (Alcalá et al. 2004; Gandolfi et al. 2008). There is indeed evidence for sequential star formation in the region, with the Orion OB stars probably being the triggering sources (Stanke et al. 2002; Gandolfi et al. 2008). Possible scenarios for triggered star formation in L 1616 have been discussed by Alcalá et al. (2004) and Gandolfi et al. (2008). Thus, unlike the fossil star forming regions in Orion, L 1616/L 1615 appear to be a region of on-going star formation relatively far from the Orion A and B clouds, in which star formation was most likely induced by the impact of the massive stars in the Orion OB association.

3.1. L1616 and L 1615: PMS Stars

The most recent and comprehensive list of PMS stars in L 1616/L 1615 is provided by Gandolfi et al. (2008). The number of confirmed PMS stars in these clouds, including the B9V-type star HD 293815 and the Herbig Ae/Be star UX Ori, sums up to 58. The coordinates and some information on these stars are provided in Table 9, while more details on their properties can be found in Gandolfi et al. (2008).

The star UX Ori, which coincides with the IR source IRAS 05020–0351, is located about $45'$ west of the L 1615, L 1616 and CB 28 clouds (see Figure 6). UX Ori is also the prototype of a class of objects with similar characteristics and that show similar behavior; it is an intermediate-mass ($M = 2.5M_{\odot}$) PMS star with spectral type A3 and age of about 2 Myr (Natta et al. 1999). Its age is consistent with that of the lower mass stars in these clouds (e.g. Alcalá et al. 2004; Gandolfi et al. 2008). The star has a strong IR excess which has been ascribed to a circumstellar disk (Hillenbrand et al. 1992). A description of this object can be found in Natta et al. (1999). UX Ori shows complex spectroscopic, photometric and polarimetric variability. This behavior is thought to arise from the fact that UX Ori and its circumstellar disk are viewed at high inclination (Natta et al. 1999; Natta & Whitney 2000). It has also been argued that the observed variability of UX Ori may be due to violent comet-like activity (see Grinin et al. 2001; Beust et al. 2001; Lagrange et al. 2000; Natta, Grinin & Mannings 2000, and references therein). The near-IR emission of UX Ori may be due to scattered light if the inner disk emission is partially obscured by an outer flared disk (Monnier et al. 2005). Extended CO emission, indicating presence of gas distant from the star, has been detected by Dent et al. (2005). Such CO emission is possibly associated with the extended far-IR emission observed by Natta et al. (1999). Testi et al. (2001) report millimeter and centimeter observations of UX Ori and propose two disk models that can explain the remarkably flat spectral index observed in the millimeter range. UX Ori has been detected by Hipparcos as a possible binary star (Bertout et al. 1999).

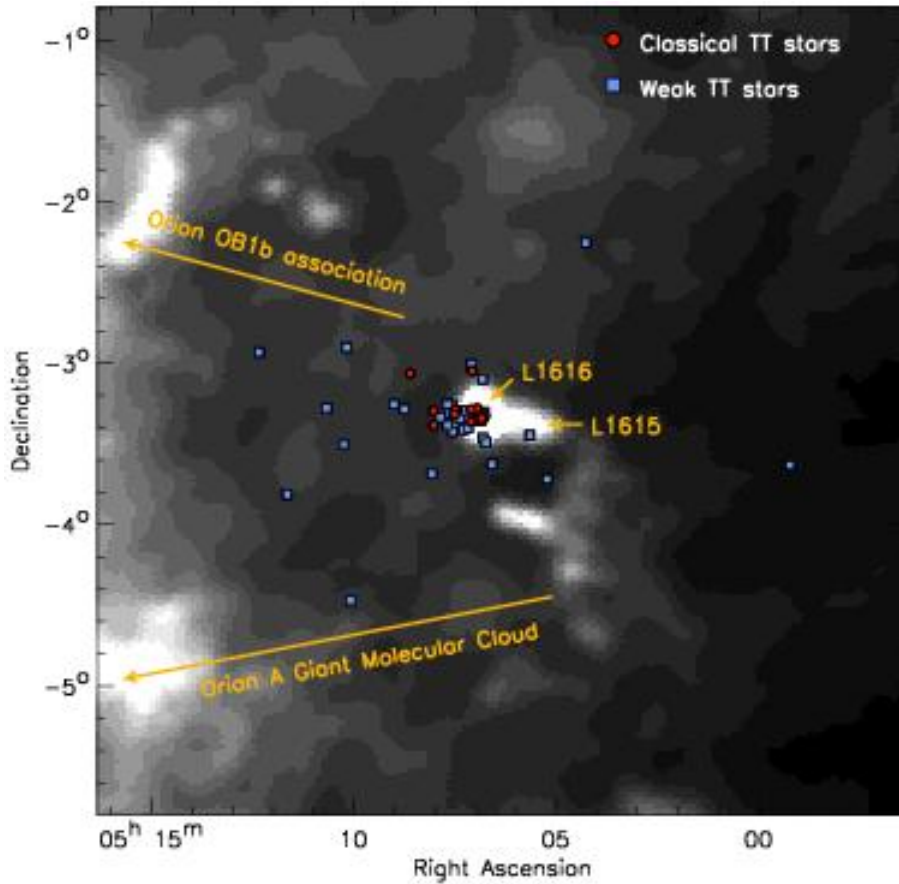


Figure 7. Spatial distribution of the PMS stars in L 1615/L 1616 overplotted on the $100\ \mu\text{m}$ IRAS map. The covered area is $5^\circ \times 5^\circ$, North is up and East to the left. The symbols represent the Classical and Weak-line T Tauri stars according to Gandolfi et al. (2008) from which the figure has been adapted here.

3.2. L1616 and L 1615: Infrared, Centimeter and Millimeter Sources

One of the most interesting IR sources in this region is IRAS 05020–0351, which coincides with the Herbig Ae/Be star UX Ori. Another one is IRAS 05044–0325, which can be identified with the $H\alpha$ -emission star Kiso A-0974 15. The other source is IRAS 05076–0257, that can be identified with the star V1011 Ori, which turned out to be a T Tauri star (Alcalá et al. 2004). Stanke et al. (2002) reported mid-infrared and 1.2 mm observations in L 1616, which revealed five MIR sources, that are associated with YSOs. Their coordinates are reported in Table 9. The 1.2 mm observations revealed a group of four dust continuum sources, whose coordinates are also reported in Table 9. The brightest millimeter source, which drives a near-IR H_2 powerful jet (see Section 3.3), may be a Class-0 protostar (Stanke et al. 2002). In addition, there are three IRAS sources close to CB 28, namely, IRAS 05038–0400, IRAS 05036–0359 and IRAS 05037–0402. The $H\alpha$ -emission star Kiso A-0974 13 is also located very close to this cloud.

Table 4. Herbig-Haro Objects in L 1616

Cloud	RA (2000) h m s	DEC(2000) ° ' "	cloud	driving source
HH 951-A	05:06:39.10	-03:20:46.0	L 1616	L 1616 MMS1 A
HH 951-B	05:06:49.70	-03:22:23.0	L 1616	L 1616 MMS1 A

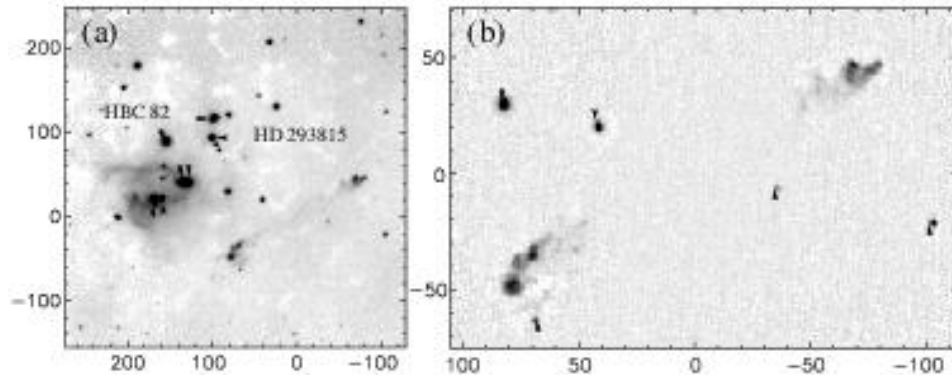


Figure 8. Infrared images of the outflow in L1616. Left panel: 2.12 μm image of the core of L 1616; diffuse H₂ emission is clearly seen just below the T Tauri star HBC 82 (=LkH α 333). Besides HBC 82 and HD 293815, the other arrows indicate the five mid-IR sources detected by Stanke et al. (2002). Right panel: enlargement of the region of the outflow. The arrows indicate stellar sources. The offsets are in arc-seconds from the position of the millimeter source L 1616 MMS1 A. The components of both HH 951-A and HH 951-B can be appreciated. Adapted from Stanke et al. (2002).

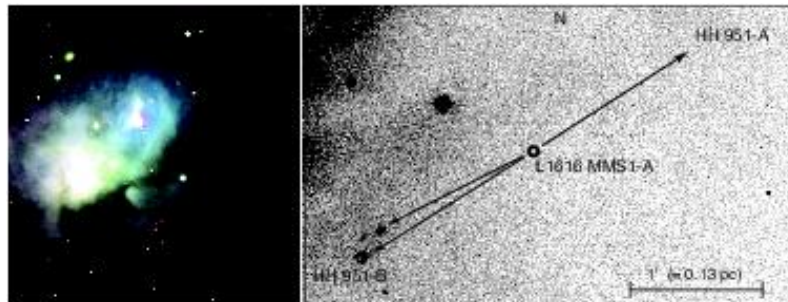


Figure 9. Optical images of the outflow in L1616. Left panel: Detail of the central part of the L 1616 image shown in Figure 5. It covers approximately the same field of view as in Figure 8 (a), i.e. about $6.7' \times 6.7'$. North is up and East to the left. The H α emission from the components of HH 951-B can be appreciated as the small red cloud fragments just below the center of the field. Right panel: a $3.4' \times 2'$ detail of the WFI H α image of the outflow in L 1616. The HH 951-B component can be clearly appreciated in the lower left. The position of the driving source is marked with the circle. HH 951-A is hidden by the high optical extinction to the west of NGC 1788.

3.3. L1616 and L 1615: Outflows and Herbig-Haro Objects

The near-IR imaging by Stanke et al. (2002) in the core of L 1616 led to the identification of three features of H_2 line emission. One of these features can be appreciated as diffuse emission that may be related to the reflection nebulosity surrounding the brightest members of the cloud (see Figure 8, left panel). As Stanke et al. mention, it is most likely that this feature is due to fluorescent emission from UV-excited H_2 in the vicinity of the most massive members of L 1616, in particular the B9 V star HD 293815.

The other two features can be clearly identified with two bow-shock structures north-west and south-east of the millimeter sources revealed in this region (cf. Figure 8). They are apparently shocks due to a protostellar outflow driven by one of the millimeter sources. Stanke et al. consider the most massive millimeter source, L 1616 MMS1-A, as the most likely driving source of the outflow. The projected length of the outflow is about $190''$, which corresponds to ~ 0.41 pc at a distance of 450 pc. Stanke et al. did not find any further emission beyond the two bow shocks. The approximate coordinates of the brightest knots in this outflow are reported in Table 4. This object has been assigned the number HH 951, following the criteria for the HH numbers designation (Reipurth 2000). HH 951-B is detected in $H\alpha$ images, but HH 951-A is barely seen in such images (see Figure 9). In addition, [S II] emission from HH 951 has been detected on an objective prism plate (Reipurth, private communication).

4. IC 2118

The IC 2118 region, also known as the *witch-head nebula*, is a long, filamentary reflection nebula, located at an angular distance of about 8 degrees west of the Orion A molecular cloud (cf. Figure 1 and 11). An optical color image of the cloud is shown in Figure 10. The cloud is also known as Ced 41 (Cederblad 1946) and Hubble 9 (Hubble 1922, catalog). IC 2118 lies far from the Orion OB1 association, clearly outside the region occupied by luminous stars, and also well separated from the Orion main molecular clouds. The supergiant star *Rigel* (β Ori), seen projected at about two degrees east of IC 2118, is thought to be the illuminating source of the nebula. A good description of the IC 2118 region and its associated clouds can be found in Kun et al. (2001).

A number of clouds and reflection nebulae are found in this region, whose positions are marked in the $100 \mu\text{m}$ IRAS map of Figure 11 while their coordinates and designations are listed in Table 5. Dorschner & Gürtler (1966) reported two reflection nebulae in this region: DG 49 and DG 52, (Dorschner & Gürtler 1963), marked by the diamonds in Figure 11, and which indicate the two biggest portions of the cloud. The Lynds (1965) catalogue contains three associated bright nebulae, namely, LBN 968, LBN 959 and LBN 975, that can be considered as sub-structures of the same cloud. Cohen (1980) found two red nebulous objects (RNO) in the region, namely RNO 36 and RNO 37. In his Table 1 he describes RNO 36 as two extremely faint, very red stars located on an emission-rim with very faint general background nebulosity present, and RNO 37 as a group of about 18 very faint, very red stars, where the dominant two are nebulous stars. Cohen performed spectroscopic observations for seven of the stars in the RNO 37 group, most of them presenting spectral types later than K5 and emission lines.

In a survey for high-latitude molecular clouds Magnani, Blitz & Mundy (1985) detected two molecular clouds in the region of IC 2118: MBM 21 and MBM 22. Ogura

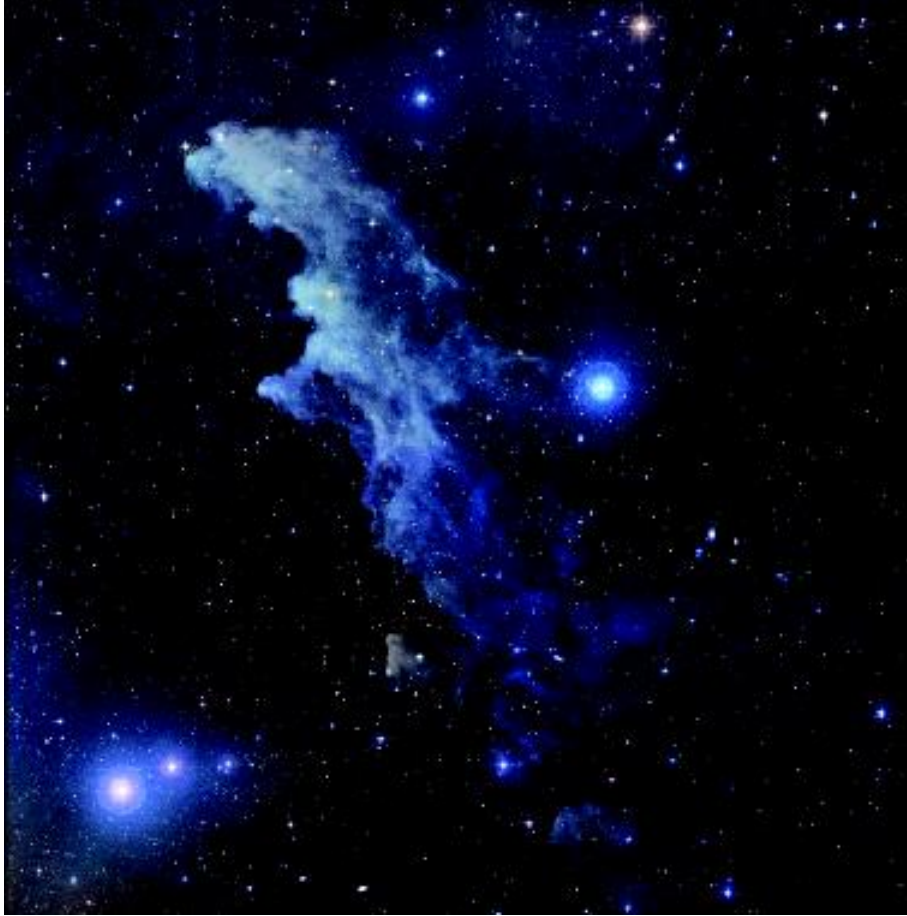


Figure 10. Optical color image of the IC 2118 region, adapted from an image by Noel Carboni. The image covers a field of about $4^\circ \times 4^\circ$; North is up and East to the left.

& Sugitani (1998) classified the clouds associated with IC 2118 as remnant molecular clouds. The clouds MBM 21 and MBM 22 were included in the IR survey by Reach, Wall & Odegard (1998). Using the NANTEN telescope Yonekura et al. (1999) investigated the molecular clouds associated with the IR sources IRAS 04591–0856 (G208.3–28.4) and IRAS 05050–0614 (G206.4–25.9) in the ^{12}CO , ^{13}CO , and C^{18}O transitions. The molecular clouds G208.3–28.4 and G206.4–25.9 detected by Yonekura et al. (1999) coincide spatially with MBM 21, investigated by Magnani, Blitz & Mundy (1985), and RNO 37 (Cohen 1980), respectively. The IRAS sources have infrared flux density distributions characteristic of YSOs, and their association with molecular clouds is a strong indication of star formation in those clouds. The ^{12}CO maps show that MBM 21 has a cometary shape with the head pointing towards the Orion OB1 association, while the ^{13}CO data indicate that such cometary structure is formed by photoevaporation (Yonekura et al. 1999).

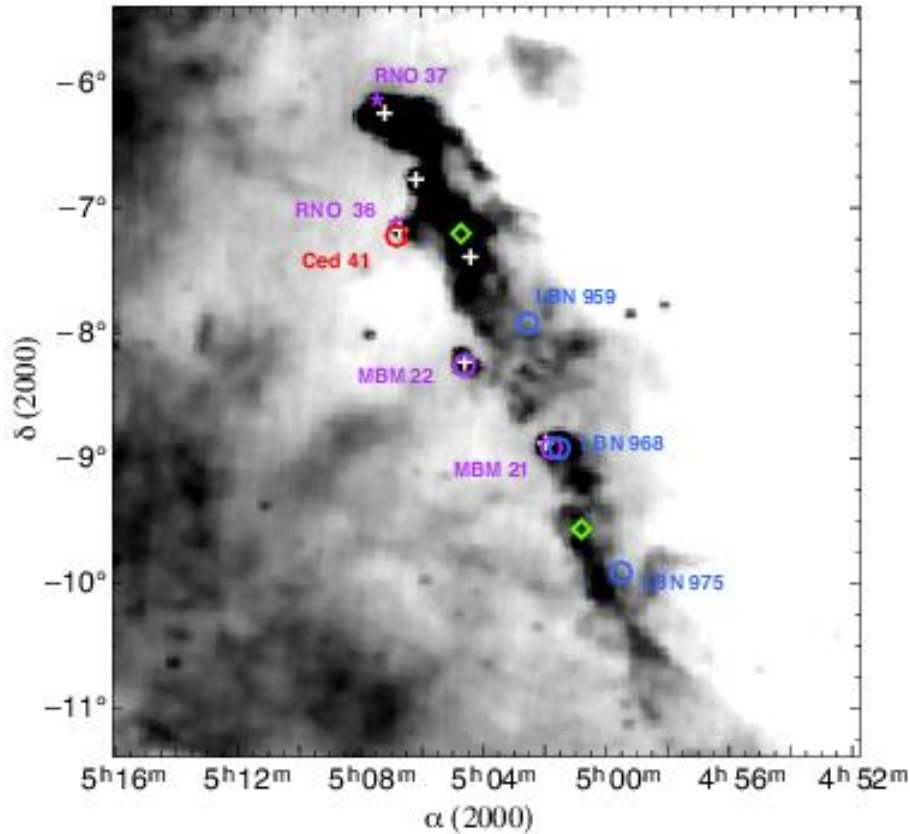


Figure 11. Map of the $100\ \mu\text{m}$ IRAS dust emission in the IC 2118 region. The positions of the clouds according to Table 5 are indicated with circles. The positions of the RNOs reported by Cohen (1980) are marked with asterisks, while the clouds detected in the CO survey by Kun et al. (2001) are represented with white *plus* symbols. The southern and northern diamonds mark the positions of the two reflection nebulae, DG 49 and DG 52 respectively, listed by Dorschner & Gürtler (1966).

Kun et al. (2001) performed a ^{12}CO survey in about 6 square-degrees in the region of IC 2118 and identified six molecular clouds, among which MBM 21 and MBM 22, as well as the other clouds discussed above, and derived the physical properties of the clouds. In Table 5 the coordinates of the clouds in the region of the reflection nebula IC 2118 are provided, together with other cloud designations, while Figure 11 shows the clouds on the $100\ \mu\text{m}$ IRAS dust emission map.

4.1. IC 2118: PMS Stars

Based on an objective-prism survey, Kun et al. (2001) identified 46 candidate emission-line stars which were more recently investigated spectroscopically by Kun et al. (2004). They identified five classical T Tauri stars in the region of IC 2118 which are listed in Table 9. Three of them were previously known IRAS sources. Using the near-IR magnitudes from the 2MASS catalogue and adopting a distance of 210 pc (see Section 8.), Kun et al. (2004) estimated, by comparison with Palla & Stahler (1999) PMS evolu-

Table 5. Coordinates of the Dark Clouds and Bright Nebulae in the IC 2118 Region.

Cloud	RA (2000) h m s	DEC(2000) ° ' "	l (°)	b (°)	other IDs	refs.
G 206.4–26.0	05:07:11	−06:15:06	206.400	−26.000		1
G 206.8–26.5	05:06:10	−06:47:01	206.800	−26.467		1
G 207.3–26.5	05:06:41	−07:11:11	207.267	−26.533	Ced 41, Hubble 9	1, 2, 3
G 207.2–27.1	05:04:25	−07:24:11	207.200	−27.133		1
G 208.1–27.5	05:04:36	−08:14:30	208.067	−27.467	MBM 22	1, 4
G 208.4–28.3	05:01:59	−08:53:18	208.400	−28.333	MBM 21	1, 4
LBN 959	05:02:34	−07:55:53	207.500	−27.780		5
LBN 968	05:01:33	−08:55:55	208.390	−28.450		5
LBN 975	04:59:32	−09:55:21	209.160	−29.330		5

References: 1: Kun et al. (2001); 2: Cederblad (1946); 3: Hubble (1922); 4: Magnani, Blitz & Mundy (1985); 5: Lynds (1965)

tionary tracks, an average age of 2.5 Myrs and masses in the interval 0.4-1.0 M_{\odot} for the members of the IC 2118 association. They concluded that the five classical T Tauri stars projected on the clouds are physically related to them, and that star formation in the region was most likely triggered by shock waves possibly originating from the Orion OB1 association. In addition, Kun et al. (2004) report other three stars that they indicate as PMS star candidates. Two of these (2MASS J05060574–0646151 and 050944864–0906065) are most likely weak-line T Tauri stars, while the other one (2MASS J05112460–0818320), showing very strong variations in its spectrum, may be a classical T Tauri star. One of the two weak-line T Tauri star candidates (2MASS J05060574–0646151) is projected on the molecular cloud G 206.4-26.0, while the other and the classical T Tauri star candidate are located far from the IC 2118 clouds. These three stars are also reported in Table 9 as T Tauri star candidates in IC 2118.

Other four T Tauri stars in the field of IC 2118 were identified as optical counterparts of ROSAT All-Sky Survey sources and their properties are reported in Alcalá, Chavarria & Terranegra (1998); Alcalá et al. (2000). Although these objects are projected relatively far from the IC 2118 clouds we also include them in Table 9 as possible members of IC 2118.

4.2. IC 2118: Infrared, Centimeter and Millimeter Sources

Early studies revealed the IR sources IRAS 05050–0614 and IRAS 04591–0856, both identified with young stars. IRAS 05050–0614 is located in the head of the northernmost part of the nebula. It is identified with the $H\alpha$ -emission star Kiso A-0974 19 and was later confirmed to be a classical T Tauri star by Kun et al. (2004) (see Table 9). More controversial was the identification of IRAS 04591–0856. Being located in the MBM 21 cloud, it coincides with a small nebulous object catalogued as a Herbig–Haro object (G 13 by Gyul’budaghian (1982); and HHL 17 by Gyul’budaghian et al. (1987)). However, its Herbig–Haro nature was not confirmed later. Persi et al. (1988) found a spectral energy distribution that is intermediate between that of a low-mass protostar and a deeply embedded T Tauri star. Analogous conclusion was reached by Tapia et al. (1997), who found that IRAS 04591–0856 is a heavily reddened ($A_V < 15$ mag) T Tauri star, but did not detect any nebulosity around the very red point-like object in

their near-IR images. Kun et al. (2001) found that the spectral energy distribution of IRAS 04591–0856 in the 1.25–100 μm wavelength range is characteristic of Class-I sources, while the optical visibility suggests a more evolved nature. Finding strong variability, Kun et al. (2001) concluded that IRAS 04591–0856 is most likely a low-mass star near the birthline. In the 2MASS images this object appears as point-like but with a surrounding nebulosity. Thus, we list this source in Table 9 as a low-mass PMS object.

Additional objects in IC 2118 come from Kun et al. (2001) who selected 11 faint IR sources from the IRAS Point Source Catalogue and Faint Source Catalogue in the region. Three of those, namely IRAS 04587–0854, IRAS F 05044–0621 and IRAS F 05047–0618, have a 2MASS counterpart; the latter two were found to be classical T Tauri stars in subsequent spectroscopic follow-up observations by Kun et al. (2004) (see Table 9). The remaining IR sources were found to be parts of small but extended structures at 12 and 25 μm , though most of them appeared to be point-like at 60 and 100 μm , suggesting that they are small-scale density or temperature enhancements in the cloud with sizes of 5'–10', corresponding to 0.3–0.6 pc at a distance of 210 pc (Kun et al. 2001).

5. L 1642

L 1642 is a well known high Galactic latitude translucent/dark cloud, also listed as MBM 20 in Magnani, Blitz & Mundy (1985). Based on previous multiwavelength data (Taylor et al. 1982; Laureijs et al. 1987; Liljeström & Mattil 1988; Liljeström 1991), L 1642 appears as a cool and quiescent cloud, associated with a much larger HI cloud (over 4 deg) with cometary structure. The tail, extending more than 5 degrees in the north-east direction, is perpendicular to the Galactic plane and points towards the plane. On the sky, L 1642 is projected in the direction of the edge of the Orion-Eridanus Bubble, with which it might be interacting (Lehtinen et al. 2004).

In general, high latitude molecular clouds are considered young and transient structures (Magnani, La Rosa & Shore 1993; Heithausen 1996) and only in rare cases these clouds show evidence of star formation. L 1642 is one of the two high-latitude ($||b|| > 30^\circ$) clouds known to have star formation (the other one is MBM 12, see Luhman 2001, and references therein).

The morphology and physical properties of L 1642 have been recently investigated by Russeil et al. (2003) in the CO, and by Reach, Wall & Odegard (1998), Verter et al. (2000) and Lehtinen et al. (2004, 2007) in the mid- and far-IR. A detailed study of the optical and IR properties of the dust grains in the region is reported in Lehtinen et al. (2007). The maximum optical extinction in the central part of the cloud has been estimated to be $A_v = 8$ mag, based on near-IR color excesses derived from 2MASS data, while an extended lower extinction halo is seen around the central core from extinction, optical scattered-light and far-IR 100 μm IRAS maps (Lehtinen et al. 2004, 2007). Large-scale mapping at 200 μm with ISO showed that the cloud consists of three separate denser regions connected by diffuse material (Lehtinen et al. 2004, 2007). Two filaments of dust extend respectively to the North-East and East from the main cloud. Only the region with the highest dust column density corresponds to a temperature minimum of 13.8 K. Close to this densest core there are two nebulous low-luminosity PMS binary stars, L 1642-1 (EW Eri) and L 1642-2 (HBC 410) both detected by IRAS (Sandell et al. 1987). Lehtinen et al. (2004) estimate that the ratio between virialized

and observed mass is about 1.2 for the densest part (region B), while for other regions it is about 10 and conclude that, within uncertainties, only region B can be gravitationally bound, while the other parts of L 1642 are transient (see Fig. 2 in Lehtinen et al. 2004). A decrease in dust temperature towards the center of the dense region B, by an amount that cannot be explained only in terms of attenuation of the radiation field, and an increase in apparent emissivity in the colder regions are observed in the cloud; these two phenomena can be explained in terms of an increase of the dust absorption cross-section at far IR wavelengths (Lehtinen et al. 2007).

5.1. L 1642: PMS Stars

There are two PMS binaries in this region: L 1642-1 and L 1642-2. L 1642-1A is optically identified as a K 7IV T Tauri star, obscured by about 2 mag of visual extinction (Sandell et al. 1987). The secondary, at 2.7 arcsec separation, appears quite bright in the far-red, and might become dominant in the IR. L 1642-2A, a faint M0 H α -emission star associated with a small compact reflection nebula, is the powering source of the Herbig-Haro object HH 123 (Reipurth & Heathcote 1990). Its secondary component, at about 5.4 arcsec separation, is also a H α -emission star, has a redder color than the primary, and might be responsible for the far-IR emission. The two components correspond altogether to the IR source IRAS 04325–1419. A small, weak molecular outflow is centered on this object (Liljeström et al. 1989). This source was also included in the 1300 μ m survey by Reipurth et al. (1993) who derived a bolometric luminosity of 0.4 L_{\odot} . Both binaries are projected on regions of high extinction, and have very low luminosity (less than about 0.5 M_{\odot} , if a distance of 100 pc is adopted). Both secondaries appear very active: L 1642-1B shows Br- γ emission, while L 1642-2B exhibits H $_2$ emission in the IR (Sandell et al. 1987).

5.2. L 1642: Infrared, Centimeter and Millimeter Sources

Apart from L 1642-1, and L 1642-2, four additional IRAS Point Source Catalogue objects also fall within the boundaries of the 200 μ m map of Lehtinen et al. (2004), e.g.: IRAS 04336–1412 (L 1642-3), IRAS 04347–1415 (L 1642-4), IRAS 04342–1444 (BD-14 929) and IRAS 04349–1436, which are detected only at 60 μ m, 100 μ m, 12 μ m and 100 μ m, respectively. None of the IRAS sources, nor any other point source candidates, is detected at 200 μ m.

5.3. L 1642: Outflows and Herbig-Haro Objects

This cloud hosts the Herbig-Haro object HH 123 ($\alpha_{2000} = 04^h34^m49.60^s$; $\delta_{2000} = -14^{\circ}13'08''0$), discovered by Reipurth & Heathcote (1990), who described it as a slightly elongated amorphous object. From their low-dispersion spectra they found that the object is of intermediate excitation with a reddening $E(B - V) \approx 0.4$. From their high-resolution spectra a number of red lines are detected which reveal three emission components with velocities of about -70, 0, and +110 km s $^{-1}$, respectively. They interpreted these components in terms of two bow shocks moving away, in opposite directions, from the source L 1642-2, which is driving the outflow.

6. Other Small Orion Outlying Clouds

Other Orion outlying clouds with much less information in the literature that we discuss briefly here are the two small clouds CB 28 and CB 29 coming from the catalogue of optically selected clouds by Clemens & Barvainis (1988), and the Lynds bright nebulae LBN 991, LBN 917, and LBN 906 (Lynds 1965).

6.1. CB 29

CB 29 is a small ($\sim 18'$; or ~ 2 pc at the distance of 460 pc) cloud that lies about 3 degrees to the west of the Orion OB1a association and about $40'$ to the north of L 1634 (see Figures 1 and 3). The properties of this cloud have been studied by Clemens & Barvainis (1988). Four IRAS sources are found closeby (e.g. IRAS 05194–0343, IRAS 05194–0346, IRAS 05201–0341 and IRAS 05190–0348), while three $H\alpha$ emission stars (e.g. Kiso A-0975 65, Kiso A-0975 66 and Kiso A-0975 67) appear projected on the cloud.

6.2. CB 28

This is the small cloud located some $25'$ south of the L 1616 cometary cloud (see Figure 6). This cloud coincides with the Lynds bright nebula LBN 923, and the object No. 67 catalogued by Lee & Myers (1999), which is considered to be a starless core. The CB 28 cloud has been studied in the IR by Reach, Wall & Odegard (1998) and in CO by Park, Lee & Myers (2004). The radial velocity of the cloud, as determined from the ^{12}CO and ^{13}CO lines reported by Park, Lee & Myers (2004), is consistent with that of the Orion giant molecular cloud.

6.3. LBN 991, LBN 917 and LBN 906

LBN 991 is located at about 8 degrees in angular distance south-west of the Orion A molecular cloud. Not much investigation has been carried out on this cloud but we decided to include it in this chapter because it coincides with one of the X-ray clumps detected in the analysis of the ROSAT All-Sky Survey X-ray sources in Orion. In the $100\ \mu\text{m}$ IRAS map LBN 991 appears as a diffuse cloud (see Figure 1).

LBN 917 and LBN 906 are some of the most distant clouds, in angular distance, from the Orion association that are discussed here (see Figure 1). LBN 917 was detected in the IR survey by Reach, Wall & Odegard (1998), who identified the clouds as DIR 203–32. Bally et al. (1991) concluded that these clouds must have been either ejected from a region near the Orion main molecular clouds or condensed from the expanding HI shell surrounding the Orion clouds. These clouds are indeed projected at an angular distance of more than 10 degrees from the Orion giant molecular cloud and are more probably related to the Orion-Eridanus bubble. Further CO observations of LBN 917 were performed by Magnani et al. (2000) and Onishi et al. (2001). Some scattered T Tauri and $H\alpha$ emission-line stars are found in the surroundings. Their coordinates are reported in Table 9.

The IRAS source IRAS 04451–0539, close to LBN 917 and LBN 906, was classified as a T Tauri star by Gregorio-Hetem et al. (1992), based on $H\alpha$ emission and strong lithium $\lambda 6708\ \text{\AA}$ absorption in its optical spectrum.

On the other hand, several RASS sources form an X-ray clump close to the LBN 991 nebula (see Figure 1). The X-ray source RX J0513.4–1244, classified as a G4

weak-line T Tauri star by Alcalá et al. (2000), and the H α -emission star Kiso A-1047-1 are projected in the proximity of the nebula, though the IR colors of the latter do not satisfy the criteria adopted by Lee et al. (2005). Therefore, there might be many more X-ray emitting PMS stars still to be discovered in this region.

6.4. Anonymous X-ray Clump

A concentration of X-ray sources that satisfy the criteria by Sterzik et al. (1995) was detected at $\alpha \approx 05^h 21^m$, $\delta \approx -09^\circ$, some 3 degrees to the south of L 1634 (see Figure 1). Several PMS stars are found in the vicinity of this clump: three are identified as optical counterparts of ROSAT All-Sky Survey sources (Alcalá et al. 1996, 2000) and one is an IRAS source (IRAS 05222–0844) classified as a T Tauri star by Gregorio-Hetem & Hetem (2002). The latter was also detected in X-rays with ROSAT (Alcalá et al. 1996, 2000). In addition, 9 Kiso H α -emission stars are found around the X-ray clump, but we do not include them in Table 9 because their IR (2MASS) colors do not satisfy the criteria for PMS stars indicated by Lee et al. (2005). Follow-up spectroscopy is needed to assess their PMS nature.

7. Small Globules around σ Ori

One of the most massive stars in Orion is the O7V star σ Ori. For a review on the cluster around this object we refer the reader to the chapter by Walter et al. in this book. In this section we discuss the four small globules No. 27, 35, 40 and 41 by Ogura & Sugitani (1998), located in the vicinity of σ Ori, and whose morphology and characteristics suggest a possible evolutionary sequence of remnant clouds, starting from bright-rimmed clouds, through cometary globules, to reflection clouds, as proposed by Ogura & Sugitani (1998). The coordinates of these globules, their approximate size and designations are listed in Table 6, while their spatial distribution relative to σ Ori is shown in Figure 12. Three of the globules (27, 35 and 40) lie to the north-west of the star, while the other one (41) is located to the south. From Figure 12 it is evident that the tails of OS98 27, OS98 35 and OS98 40 point away from σ Ori, which underlines the impact of the strong wind from the massive star on these globules. There is evidence of recent or ongoing star formation in these clouds. A discussion cloud by cloud is presented below and, as a reference, optical color images of each globule are shown in Figure 13.

Table 6. Small Globules around σ Ori discussed in this Chapter.

OS98 [†]	$\alpha(2000)$ h m s	$\delta(2000)$ ° ' "	Approx. Size (arcmin)	other IDs	refs.
27	05:33:24	−00:38:03	3×5	IC 423, CB 31, LBN 913, DG 58	1, 2, 3
35	05:36:30	−00:17:26	6×4	IC 426, CB 32, LBN 921, DG 61	1, 2, 3
40	05:38:06	−01:45:29	3×5	Ori I-2, BRC 20	2, 4, 5
41	05:38:24	−05:13:49	3×8	BRC 22	4

[†] Cloud number by Ogura & Sugitani (1998)

References: 1: Dreyer (1908): *Index Catalog*; 2: Clemens & Barvainis (1988); 3: Lynds (1962); 4: Sugitani, Fukui & Ogura (1991); 5: Cernicharo et al. (1992);

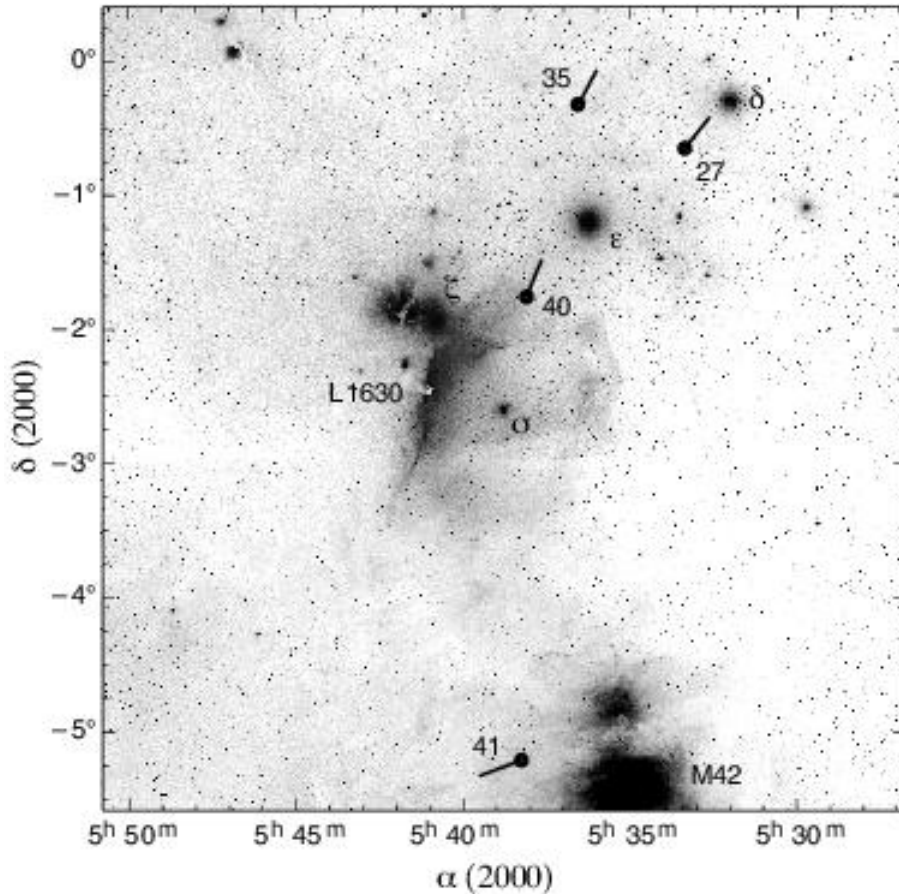


Figure 12. Spatial distribution of the small globules around σ Ori discussed in the text overlaid on the red digitized sky survey image. σ Ori is at the center of the image. The Orion belt stars are identified by the greek letters while the numbers indicate the globules according to the designation by Ogura & Sugitani (1998). Their positions are marked by black dots with pointers indicating the direction of their tails. The Orion nebula (M42) and the Horsehead nebula (L1630) are also indicated.

7.1. OS98-27

This small globule has the typical morphology of a cometary cloud with its tail pointing towards north-west. There is evidence of star formation with at least two confirmed classical T Tauri stars, namely CVSO 121 and YSO CB031YC1. These two objects were found to possess strong $H\alpha$ in emission, as well as strong lithium $\lambda 6708 \text{ \AA}$ absorption in their spectrum by Briceño et al. (2005) for the former and by Yun et al. (1997) for the latter. While CVSO 121 is located ~ 3 arc-min. to the east of the head of the cometary cloud, YSO CB031YC1 is on the tail of the cloud (see the left upper panel of Figure 13). In addition, the emission line star Kiso A-0904 10, is located to the north-west of the globule. These objects are also listed in Table 9.

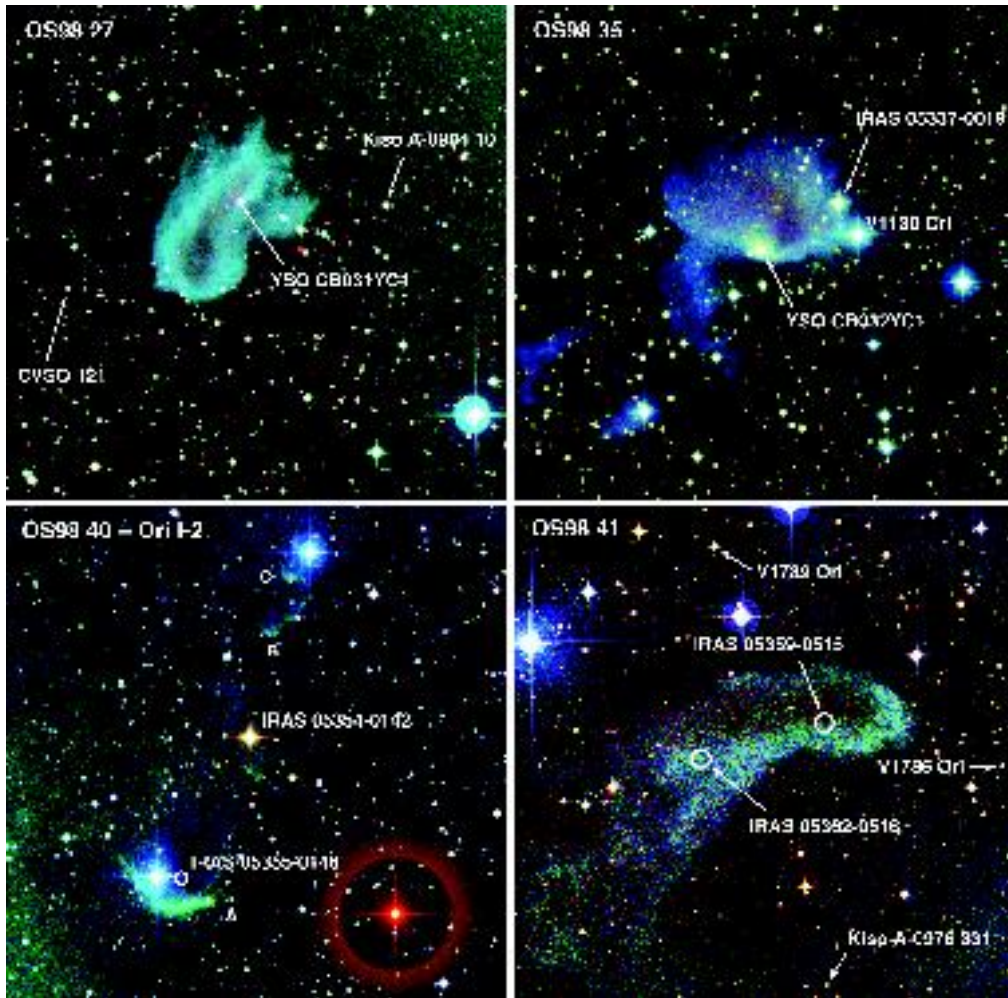


Figure 13. Optical color images of the four small globules around σ -Ori discussed in the text. The images were produced by the authors using the publicly available blue, red and IR digitized sky survey plates. Some of the most relevant objects are indicated and the position of some of the IRAS sources are marked with circles. Each image covers a field of about $15' \times 15'$, with North up and East to the left.

7.2. OS98-35

Several cloud fragments were identified by Ogura & Sugitani (1998) in this region. The most prominent is OS98-35A. Although more extended in the east-west direction, this globule also shows the typical morphology of the head of a cometary cloud. There is also evidence of star formation in this cloud: the star YSO CB032YC1, spectroscopically confirmed to be a T Tauri by Yun et al. (1997), is located at the apex of the cloud rim (see upper right panel in Figure 13). Yun et al. (1997) do not provide the optical magnitudes for this object, but we estimate $V \approx 14$. The ROSAT X-ray source 1RXS J053631.1-001744 is about 1 arc-min to the north of the T Tauri star. The source IRAS 05337-0019 is located on the western edge of OS98-35A and coincides with

the star TYC 4766-2306-1. The latter is at less than 20 arc-sec from the ROSAT X-ray source 1RXS J053620.0-001708. Given the typical error circle of the ROSAT sources, with a radius on the order of 30 arc-sec, the star may be associated with the X-ray source. However, spectroscopic evidence of the young nature of this object is missing. Hence it is listed among candidates in Table 9. Finally, the unrelated variable star V1130 Ori is also projected on the border of the OS98-35 nebulosity.

7.3. OS98-40

This cloud, projected closer to σ Ori than OS98-27 and OS98-35 (cf. Figure 12), is also very well known as Ori I-2. A detailed study of Ori I-2, including its kinematics, was conducted by Cernicharo et al. (1992) using CO observations. The three cloud fragments A, B, and C, as identified by Ogura & Sugitani (1998), are marked on the image of the cloud shown in the lower left panel of Figure 13. The most prominent of the three is fragment A, but the "V-shape" morphology of the three cloud fragments puts in evidence the interaction of the strong wind from σ Ori with the cloud material (cf. Cernicharo et al. 1992). The bright and very red star in the lower right corner of this image is the unrelated Mira variable X Ori.

A radio source, Ori-I-2 1, detected by Bontemps (1996), is located just on the apex of cloud A. The source IRAS 05355–0146 is located in the cavity of this cloud and the closeby bright star to the east is HD 37389, an unrelated B9-A0V star (Cernicharo et al. 1992). The IRAS source has been associated with an H₂O maser (Wouterloot & Walmsley 1986; Codella et al. 1995) and is the driving source of the HH 289 outflow (see below). Four emission line stars (OriI-2N-1, 2, 3, and 4) in the northern part of the globule, east of cloud C, have been discovered by Ogura, Sugitani & Pickles (2002). The northernmost of those coincides with 2MASS J05380259-0134392.

Based on CO observations Sugitani et al. (1989) found a molecular outflow around IRAS 05355–0146, which was identified as the driving source. The outflow was studied in detail by Cernicharo et al. (1992) and was later identified with HH 289 by Mader et al. (1999) using optical and infrared observations. Such images revealed a series of bowshocks in the east-west direction around IRAS 05355–0146, further confirming that the IRAS source is driving the outflow². The latter authors also concluded that the size of the outflow is slightly larger than 1 parsec, including it in the class of the parsec-scale flows.

All the above signatures testify that star formation in this region may have been triggered by the impact of hot star winds from σ Ori.

7.4. OS98-41

This cloud lies about 50 arc-min east of the Trapezium cluster (see Figure 12). Its cometary tail points eastward, indicating that the stars of the Trapezium are probably blowing the cloud material away. There is a large number of Parenago stars in the field of this cloud that have been studied photometrically by Rebull et al. (2000), but no spectroscopic evidence of their youth is available. Other emission-line and variable stars, like Haro 4-107 (= Kiso A-0976 331) and V1786 Ori, lie in the field of this cloud. The sources IRAS 05359-0515 and IRAS 05362-0516 are located in the body of the cloud, which is usually identified with the former.

²Note that in Mader et al. (1999) IRAS 05355-0146 is erroneously reported as IRAS 05355–0416.

8. Cloud Distances

So far there is not much data on the distances of the Orion outlying clouds. For some of the clouds the distance to the Orion nebula cluster is normally assumed³. A summary of the available information is given in Table 7, accompanied by a brief presentation of each individual cloud.

Table 7. Distance of the Orion Outlying Clouds.

Cloud	Distance [pc]	comments	refs.
CB 29	460-500	assumed to be the same as L 1634	
L 1634	460-500		1
L 1616 [†]	450	based on HD 293815 distance	
L 1615 [†]	450	based on HD 293815 distance	
CB 28	450	assumed to be the same as L 1615 and L 1616	
IC 2118	200-230	MBM 21	2, 3, 4
LBN 991 [†]	?		
LBN 917	100-200		
LBN 906	100-200		
L 1642 [†]	100-160	LBN 981, MBM 20	5, 3, 6

[†] coinciding with an X-ray clump (see Sect. 1).

References: 1: Fukui (1989); 2: Franco (1989); 3: Penprase (1993); 4: Kun et al. (2001); 5: Penprase (1992); 6: Hearty et al. (2000)

L 1634, CB 29: It has been assumed that L 1634 is at a distance of 500 pc (Fukui 1989). Bohigas, Persi & Tapia (1993) argued that L 1634 is a typical young cloud in Orion and adopted a distance of 460 pc. However, no direct determinations of the distance to these clouds are available so far.

L 1616, L 1615, CB 28: there are no direct determinations of the distance to these clouds. However, the distance of the B9V star HD 293815 in L 1616, is 450 pc (Warren & Hesser 1978). Moreover, the isochronal age of 1-2 Myr derived by Alcalá et al. (2004); Gandolfi et al. (2008) for the stars in L 1616 is consistent with the PMS evolution time of a ZAMS star like HD 293815, when adopting the distance of 450 pc. This provides further support for the distance of these clouds to be about 450 pc.

IC 2118: Kun et al. (2001) argued a distance of 210 pc for the clouds in this region based on several indications. In particular, the studies by Franco (1989) and Penprase (1993) of the MBM 21 cloud suggested a distance of that order. Moreover, the B8Ia-type supergiant *Rigel*, which is thought to be the illuminating source of the reflection nebula, is at a distance of 236 pc. It is thus reasonable that the distance of the IC 2118 clouds is in the range between 200 and 230 pc.

³Note that the distance of 414 ± 7 pc has been recently reported by Menten et al. (2007) for the Orion nebula cluster, which is about 10% less than the canonical value.

L 1642: The distance to L 1642 has been derived using different techniques. Magnani & de Vries (1986), from star counts, estimated a distance of 75–125 pc. Penprase (1992) derived a photometric distance between 100 and 120 pc. Using ROSAT observations, Kuntz et al. (1997) reported on the possible detection of a 0.25 keV X-ray shadow due to the cloud and suggested that L 1642 is within or close to the edge of the Local Bubble, which in that direction is at about 140 pc, according to Sfeir et al. (1999). The spectroscopic technique was also used to look for interstellar Na I D lines signature in bright stars in the direction of the cloud. Penprase (1993), using spectroscopic parallaxes of foreground and background stars to the cloud, derived an upper limit to the distance of about 110 pc, while Hearty et al. (2000), using trigonometric parallaxes measured by the Hipparcos satellite, derived a distance between 112 ± 15 pc and 161 ± 21 pc.

LBN 917, LBN 906, LBN 991: The distance to these clouds is not known. However, at least in the case of LBN 917 and LBN 906, there are evidences showing that they might be located inside the Orion-Eridanus Bubble. (Bally et al. 1991; Brown, Hartmann & Burton 1995). It thus seems reasonable that the distance of these two clouds be in the range between 100 and 200 pc.

9. Summary

As a summary we present in Table 8 the numbers of YSOs and outflows in each region discusses above and a bibliographic guide to the observational studies performed in different wavelength ranges.

The apparent small number of YSOs found so far in the region of L 1634 compared to L 1616 may result from the fact that the studies conducted in this region have been mainly devoted to the investigation of the outflow, rather than to the search of PMS stars. Many more low-mass PMS stars in L 1634 are hence expected to be identified in the coming years. It is not surprising that the clouds with most active star formation are closer in angular distance to the main Orion molecular clouds, in particular L 1634, L 1615 and L 1616. Star formation in the IC 2118 region is also ongoing, although not so vigorously as in L 1616. IC 2118 may be connected to the star-forming complex in Orion. However, a true link has not been clarified yet. Given the distance of 210 pc for the reflection nebula and its associated molecular clouds, the stellar association in IC 2118 may be located within the Orion–Eridanus Bubble (Kun et al. 2004). The other clouds at higher galactic latitude, like L 1642, are probably related to the Orion-Eridanus bubble rather than to the Orion star forming region. In fact, those clouds are closer to the Sun, consistently with the idea that they may be associated with the nearest side of the bubble outskirts. Further investigations of the PMS populations of these clouds in the coming years will help to shed light on their relationship with the Orion-Eridanus bubble.

Table 8. Summary of observations in the Orion outlying clouds and other globules

Cloud	Number of		X-rays	optical	References	
	YSOs	outflows			IR	radio
L 1634, CB 29	9	2	15, 16	1, 5, 10 12, 16, 43	2, 10, 13, 17, 24, 29, 44	3, 22, 23, 4, 7, 17
L 1616 and 1615, CB 28	57	1	15, 16	16, 37, 43	16, 25, 30, 37	25, 7, 14, 32
IC 2118	10		15, 16	16, 26, 43	21, 30	31, 4, 9, 21
LBN 991	1		15, 16	16	–	–
LBN 917, LBN 906	1		15	11	30	9
L 1642	6	1	15	6, 18, 19	20, 28, 30	3, 4, 27
anonymous X-ray clump	4		15, 16	16	–	–
OS98-27	2			33, 34	–	–
OS98-35	1			33	–	–
OS98-40 = Ori I-2	1	1	38	35, 40	35, 42	36, 39, 40, 41

1: Cohen (1980); 2: Cohen, Harvey & Schwartz (1985); 3: Magnani, Blitz & Mundy (1985);
4: Maddalena et al (1986); 5: Stephenson (1986); 6: Sandell et al. (1987); 7: Clemens & Barvainis
(1988); 8: Reipurth & Heathcote (1990); 9: Bally et al. (1991); 10: Sugitani, Fukui & Ogura (1991);
11: Gregorio-Hetem et al. (1992); 12: Bohigas, Persi & Tapia (1993); 13: Hodapp & Ladd (1995);
14: Ramesh (1995); 15: Sterzik et al. (1995); 16: Alcalá et al. (1996, 2000, 2004); 17: Davis et al. (1997);
18: Hearty et al. (2000); 19: Li et al. (2000); 20: Verter et al. (2000); 21: Kun et al. (2001); 22: Beltrán et
al. (2002); 23: De Vries et al. (2002); 24: Nisini et al. (2002); 25: Stanke et al. (2002); 26: Kun et al.
(2004); 27: Russeil et al. (2003); 28: Lehtinen et al. (2004); 29: O’Connell et al. (2004); 30: Reach, Wall
& Odegard (1998); 31: Yonekura et al. (1999); 32: Park, Lee & Myers (2004); 33: Yun et al. (1997);
34: Briceño et al. (2005); 35: Mader et al. (1999); 36: Sugitani et al. (1989); 37: Gandolfi et al. (2008);
38: Carkner et al. (1998); 39: Larionov et al. (1999); 40: Cernicharo et al. (1992); 41: Bontemps (1996);
42: Hodapp (1994); 43: Lee & Chen (2007); 44: Seale & Looney (2008)

Acknowledgements. We thank the referee, K. Sugitani, for his careful reading and helpful comments and suggestions. We are also grateful to Bo Reipurth for his manifold inputs and comments on an earlier version of the manuscript. We thank T. Stanke and C. Davis for providing figures from their work. We are grateful to Steve Rodney for his help with LaTeX and the scaling of the format of some of the figures. We also thank A. Frasca, L. Spezzi, D. Gandolfi, E. Marilli, L. Testi and A. Natta for fruitful discussions, as well as for their collaboration in some of the works mentioned in this chapter. We acknowledge the use of the color image of IC 2118 by Noel Carboni. This work was partially financed by the Italian Ministry of University and Research (MIUR). Financial support from INAF (PRIN-INAF-2005 project ”Stellar clusters: a benchmark for star formation and stellar evolution”) and from *Regione Campania* is also acknowledged. This research has made use of the SIMBAD database, operated at CDS, Strasbourg, France.

References

- Alcalá, J.M., Terranegra, L., Wichmann, R. et al. 1996, A&AS, 119, 7
- Alcalá, J.M., Chavarría-K., C. & Terranegra, L. 1998, A&A, 330, 1017
- Alcalá, J.M., Covino, E., Torres G. et al. 2000, A&A, 353, 186
- Alcalá, J.M., Watcher, S., Covino, E. et al. 2004, A&A, 416, 677
- Bally, J., Langer, W. D., Wilson, R. W., Stark, A. A., & Pound, M. W. 1991, IAU Symp. 147 *Fragmentation of Molecular Clouds and Star Formation*, eds. E. Falgarone, F. Boulanger, & G. Duvert, p. 11
- Baraffe, I., Chabrier, G., Allard, F., & Hauschildt, P. H. 1998, A&A, 337, 403
- Beltrán, M. T., Estalella, R., Ho, P. T. P., et al. 2002, ApJ, 565, 1069
- Bertout, C., Robichon, N., & Arenou, F. 1999, A&A, 352, 574
- Beust, H., Karmann, C., & Lagrange, A.-M. 2001, A&A, 366, 945
- Bohigas, J., Persi, P., & Tapia, M. 1993, A&A, 267, 168
- Bontemps, S. 1996 Ph.D. Thesis, Univ. Paris XI
- Briceño, C., Calvet, N., Hernandez, J., Vivas, A.K., Hartmann, L., et al. 2005, AJ, 129, 907
- Brown, A. G. A., Hartmann, D., & Burton, W. B. 1995, A&A, 300, 903
- Carkner, L., Kozak, J.A., and Feigelson, E.D. 1998, AJ, 116, 1933
- Cederblad, S. 1946, Meddelanden fran Lunds Astronomiska Observatorium Serie II, 119, 1
- Cernicharo, J., Bachiller, R., Duvert, G., Gonzalez-Alfonso, E., Gomez-Gonzalez, J. 1992, A&A, 261, 589
- Chavarría-K, C., Terranegra, L., Moreno-Corral, M.A. & De Lara, E. 2000, A&AS, 145, 187
- Cieslinski, D., Jablonski, F.J., & Steiner, J.E. 1997, A&AS, 124, 55
- Clemens, D. P., & Barvainis, R. 1988, ApJS, 68, 257
- Cohen, M. 1980, AJ, 85, 29
- Cohen, M., Harvey, P. M., & Schwartz, R. D. 1985, ApJ, 296, 633
- Cohen, M., Tielens, A.G.G.M., Bregman, J. et al. 1989, ApJ, 341, 246
- Codella, C., Palumbo, G.G.C., Pareschi, G., Scappini, F., Caselli, P. et al. 1995, MNRAS, 276, 57
- Cruz, K. L., Reid, I. N., Liebert, J., Kirkpatrick, J. D., & Lowrance, P. J. 2003, AJ, 126, 2421
- Davis, C. J., Ray, T. P., Eisloffel, J., & Corcoran, D. 1997, A&A, 324, 263
- Dent, W. R. F., Greaves, J. S., & Coulson, I. M. 2005, MNRAS, 359, 663
- De Vries, C. H., Narayanan, G., & Snell, R. L. 2002, ApJ, 577, 798
- de Winter, D., Grady, C. A., van den Ancker, M. E., Pérez, M. R., & Eiroa, C. 1999, A&A, 343, 137
- Dolan, C. J., & Mathieu, R. D. 2002, AJ, 123, 387
- Dorschner, J. & Gürtler, J. 1963, Astron. Nach., 287, 257
- Dorschner, J. & Gürtler, J. 1966, Astron. Nach., 289, 57
- Downes, R.A. & Keyes, C.D. 1988, AJ, 96, 777
- Dreyer, J.L.E. 1908, MNRAS, 59, 105
- Ducourant, C., Teixeira, R., Perie, J. P., Lecampion, J. F., Guibert, J., & Sartori, M. J. 2005, A&A, 438, 769
- Franco, G. A. P. 1989, A&A, 223, 313
- Fukui, Y. 1989, in ESO Workshop *Low Mass Star Formation and Pre-main Sequence Objects*, ed. Bo Reipurth, p. 95
- Gandolfi, D., Alcalá, J.M., Leccia, S., Frasca, A., Spezzi, L., et al. 2008, ApJ, in press (arXiv0807.0532)
- Gregorio-Hetem, J., Lepine, J. R. D., Quast, G. R., Torres, C. A. O., & de La Reza, R. 1992, AJ, 103, 549
- Gregorio-Hetem, J. & Hetem, A. 2002, MNRAS, 336, 197
- Grinin, V. P., Kozlova, O. V., Natta, A., Ilyin, I., Tuominen, I., Rostopchina, A. N., & Shakhovskoy, D. N. 2001, A&A, 379, 482
- Gyul'budaghian, A. L. 1982, Pis'ma v Astronomicheskii Zhurnal, vol. 8, 232
- Gyul'budaghian, A. L., Rodríguez, F.L., Mendoza-Torres, E., 1987, Rev. Mex. Astron. Astrofis., 15, 53

- Gyul'budaghian, A. L. & Magakian, T. Y. 1977, *Soviet Astronomy Letters*, 3, 58
- Haro, G. 1949, *AJ*, 54, 188
- Hearby, T., Fernández, M., Alcalá, J. M., Covino, E., & Neuhäuser, R. 2000, *A&A*, 357, 681
- Heithausen, A. 1996, *A&A*, 314, 251
- Herbig, G.H. & Bell, K.R. 1988, *Lick Obs. Bull.* 1111
- Hillenbrand, L. A., Strom, S. E., Vrba, F. J., & Keene, J. 1992, *ApJ*, 397, 613
- Hodapp, K.-W., 1994, *ApJS*, 94, 615
- Hodapp, K.-W. & Ladd, E. F. 1995, *ApJ*, 453, 715
- Hubble, E. P. 1922, *ApJ*, 56, 162
- Kinnunen, T. & Skiff, B.A. 2000, *IBVS*, 4879, 1
- Kun, M., Aoyama, H., Yoshikawa, N., et al. 2001, *PASJ*, 53, 1063
- Kun, M. & Nikolic, S. 2003, *The Interaction of Stars with their Environment II*, eds. Cs. Kiss, M. Kun, & V. Könyves, Konkoly Observatory, Budapest p. 19
- Kun, M., Prusti, T., Nikolić, S., Johansson, L. E. B., & Walton, N. A. 2004, *A&A*, 418, 89
- Kuntz, K. D., Snowden, S. L., & Verter, F. 1997, *ApJ*, 484, 245
- Lada, C.J. & Lada, E.A., *ARA&A*, 41, 57
- Lagrange, A.-M., Backman, D. E., & Artymowicz, P. 2000, *Protostars and Planets IV*, Tucson: University of Arizona Press; eds. Mannings, V., Boss, A.P., Russell, S.S., p. 639
- Larionov, G. M., Val'ts, I. E., Winnberg, A., Johansson, L. E. B., Booth, R. S., Golubev, V. V. 1999, *A&AS*, 139, 257
- Laureijs, R. J., Mattila, K., & Schnur, G. 1987, *A&A*, 184, 269
- Lee, C. W. & Myers, P. C. 1999, *ApJS*, 123, 233
- Lee, H.-T., Chen, W. P., Zhang, Z.-W., & Hu, J.-Y. 2005, *ApJ*, 624, 808
- Lee, H.-T. & Chen, W. P. 2007, *ApJ*, 657, 884
- Lehtinen, K., Russeil, D., Juvela, M., Mattila, K., & Lemke, D. 2004, *A&A*, 423, 975
- Lehtinen, K., Juvela, M., Mattila, K., Lemke, D., Russeil, D. 2007, *A&A*, 466, 969
- Li, J. Z., Hu, J. Y., & Chen, W. P. 2000, *A&A*, 356, 157
- Liljeström, T. & Mattila, K. 1988, *A&A*, 196, 243
- Liljeström, T., Mattila, K., & Friberg, P. 1989, *A&A*, 210, 337
- Liljeström, T. 1991, *A&A*, 244, 483
- Luhman, K. L. 2001, *ApJ*, 560, 287
- Lynds, B. T. 1962, *ApJS*, 7, 1
- Lynds, B. T. 1965, *ApJS*, 12, 163
- Maddalena, R. J., Moscovitz, J., Thaddeus, P., & Morris, M. 1986, *ApJ*, 303, 375
- Mader, S.L., Zealey, W.J., Parker, Q.A., and Masheded, M.R.W. 1999, *MNRAS*, 310, 331
- Magakian T.Y. 2003, *A&A*, 399, 141
- Magnani, L., Blitz, L., & Mundy, L. 1985, *ApJ*, 295, 402
- Magnani, L. & de Vries, C. P. 1986, *A&A*, 168, 271
- Magnani, L., LaRosa, T. N., & Shore, S. N. 1993, *ApJ*, 402, 226
- Magnani, L., Caillault, J.-P., Buchalter, A., & Beichman, C. A. 1995, *ApJS*, 96, 159
- Magnani, L., Hartmann, D., Holcomb, S.L., Smith, L.E., Thaddeus, P. 2000, *ApJ*, 535, 167
- Maheswar, G., Manoj, P. & Bhatt, H.C. 2003, *A&A*, 402, 963
- Menten, K.M., Reid, M.J., Forbrich, J., and Brunthaler, A. 2007, *A&A*, 474, 515
- Monnier, J. D., Millan-Gabet, R., Billmeier, R., Akeson, R. L., Wallace, D., et al. 2005, *ApJ*, 624, 832
- Nakano, M., Wiramihardja, S.D., & Kogure, T. 1995, *PASJ*, 47, 889
- Nesterov, V.V., Kuzmin, A.V., Ashimbaeva, N.T. et al. 1995, *A&AS*, 110,367
- Natta, A., Prusti, T., Neri, R., Thi, W. F., Grinin, V. P., & Mannings, V. 1999, *A&A*, 350, 541
- Natta, A., Grinin, V. P., & Tambovtseva, L. V. 2000, *ApJ*, 542, 421
- Natta, A., Grinin, V., & Mannings, V. 2000, *Protostars and Planets IV*, Tucson: University of Arizona Press; eds. Mannings, V., Boss, A.P., Russell, S.S., p. 559
- Natta, A. & Whitney, B. A. 2000, *A&A*, 364, 633
- Nisini, B., Caratti o Garatti, A., Giannini, T., & Lorenzetti, D. 2002, *A&A*, 393, 1035
- O'Connell, B., Smith, M. D., Davis, C. J., Hodapp, K. W., Khanzadyan, T., & Ray, T. 2004, *A&A*, 419, 975

- Ogura, K. & Sugitani, K. 1998, *Pub. Astron. Soc. Australia*, 15, 91
- Ogura, K., Sugitani, K., & Pickles, A. 2002, *AJ*, 123, 2597
- Olnon, F.M., Raimond, E., & IRAS Science Team 1986, *A&AS*, 65, 607
- Onishi, T., Yoshikawa, N., Yamamoto, H., et al. 2001, *PASJ*, 53, 1017
- Osterloh, M. & Beckwith, S. V. W. 1995, *ApJ*, 439, 288
- Palla, F. & Stahler, S. W. 1999, *ApJ*, 525, 772
- Park, Y.-S., Lee, C. W., & Myers, P. C. 2004, *ApJS*, 152, 81
- Parsamian, E. S., & Petrosian, V. M. 1979, *Soobshcheniya Byurakanskoj Observatorii Akademii Nauk Armyanskoj SSR Erevan*, 51, 3; *ibidem*, 51, 12
- Penprase, B. E. 1992, *ApJS*, 83, 273
- Penprase, B. E. 1993, *ApJS*, 88, 433
- Persi, P., Ferrari-Toniolo, M., Busso, M., Robberto, M., Scaltriti, F., & Silvestro, G. 1988, *AJ*, 95, 1167
- Ramesh, B. 1995, *MNRAS*, 276, 923
- Reach, W.T., Wall, W.F., & Odegard N. 1998, *ApJ*, 507, 507
- Rebull, L.M., Hillenbrand, L.A., Strom, S.E., Duncan, D.K., Patten, B.M., et al. 2000, *AJ*, 119, 3026
- Reipurth, B. 2000, *A General Catalogue of Herbig-Haro Objects*, *VizieR Online Data Catalog*, 5104
- Reipurth, B. & Heathcote, S. 1990, *A&A*, 229, 527
- Reipurth, B., Chini, R., Krugel, E., Kreysa, E., & Sievers, A. 1993, *A&A*, 273, 221
- Reipurth, B. & Zinnecker, H. 1993, *A&A*, 278, 81
- Russeil, D., Juvela, M., Lehtinen, K., Mattila, K., & Paatero, P. 2003, *A&A*, 409, 135
- Sandell, G., Reipurth, B., & Gahm, G. 1987, *A&A*, 181, 283
- Seale, J.P. & Looney, L.W. 2008, *ApJ*, 675, 427
- Sfeir, D. M., Lallement, R., Crifo, F., & Welsh, B. Y. 1999, *A&A*, 346, 785
- Stanke, T., Smith, M.D., Gredel, R., & Szokoly, G. 2002, *A&A*, 393, 251
- Stephenson, C.B. 1986, *ApJ*, 300, 779
- Sterzik, M. F., Alcalá, J. M., Neuhäuser, R., & Schmitt, J. H. M. M. 1995, *A&A*, 297, 418
- Sterzik, M. F. & Durisen, R. H. 2003, *A&A*, 400, 1031
- Sugitani, K., Fukui, Y., Mizuni, A., Ohashi, N. 1989, *ApJ*, 342, L87
- Sugitani, K., Fukui, Y., & Ogura, K. 1991, *ApJS*, 77, 59
- Sugitani, K. & Ogura, K. 1994, *ApJS*, 92, 163
- Tapia, M., Persi, P., Bohigas, J., & Ferrari-Toniolo, M. 1997, *AJ*, 113, 1769
- Taylor, M. I., Taylor, K. N. R., & Vaile, R. A. 1982, *Proc. Astron. Soc. Australia*, 4, 440
- Testi, L., Natta, A., Shepherd, D. S., & Wilner, D. J. 2001, *ApJ*, 554, 1087
- Torrelles, J. M., Rodriguez, L. F., Canto, J., Marcaide, J., & Gyulbudaghian, A. L. 1983, *Rev. Mex. Astron. Astrofis.*, 8, 147
- Verter, F., Magnani, L., Dwek, E., & Rickard, L. J. 2000, *ApJ*, 536, 831
- Walter, F. M., Alcalá, J. M., Neuhäuser, R., Sterzik, M., & Wolk, S. J. 2000, *Protostars and Planets IV*, Tucson: University of Arizona Press; eds. Mannings, V., Boss, A.P., Russell, S.S., p. 273
- Warren Jr., W. H. & Hesser, J. E., 1978, *ApJS*, 36, 497
- Weaver, W.B. & Jones G. 1992, *ApJS*, 78, 239
- Wiramihardja, S.D., Kogure, T., Yoshida, S., Ogura, K., and Nakano, M. 1989, *PASJ*, 41, 155
- Wiramihardja, S.D., Kogure, T., Yoshida, S. et al. 1991, *PASJ*, 43, 27
- Wouterloot, J.G.A. & Walmsley, C.M. 1986, *A&A*, 168, 237
- Yonekura, Y., Hayakawa, T., Mizuno, N., et al. 1999, *PASJ*, 51, 837
- Yun, J.L., Moreira, M.C., Alves, J.F. & Storm, J. 1997, *A&A*, 320, 167

Table 9. Young stellar objects in the Orion outlying clouds

Clouds / Identifier	α (2000) h m s	δ (2000) ° ′ ″	V	Sp. Type	Other Ids.	Refs.
L 1634 and CB 29:						
StHA 36	05:17:46.75	-03:58:47.0	13.00			1, 2, 3
RX J0517.9-0708 †	05:17:55.00	-07:08:25.0	10.70	K2		4, 5, 6
IRAS 05173-0555	05:19:48.90	-05:52:05.0	—		VLA 3	7, 8, 44
LDN 1634 7	05:19:51.60	-05:52:06.1	—			7, 8, 44
StHA 37	05:20:19.46	-05:45:55.4	13.31		HBC 83, Kiso A-0975 52, IRAS 05178-0548	1, 9, 10, 11, 3, 43
StHA 38 †	05:20:25.75	-05:47:06.4	14.50		V 534 Ori, Kiso A-0975 54	1, 12, 10, 2, 3, 43
StHA 39	05:20:31.43	-05:48:24.6	13.50		RX J0520.5-0548	1, 6, 2, 3, 43
RX J0520.9-0452	05:20:56.00	-04:52:43.0	9.53	F7		4, 5, 6
Kiso A-0975 69 †	05:23:03.20	-04:40:37.0	14.68	K6	RX J0523.1-0440	10, 6, 4, 13
<i>Candidates:</i>						
Kiso A-0975 40	05:17:52.25	-03:26:01.0	18.00			10
Kiso A-0975 43	05:18:16.85	-05:37:30.0	15.70			10
Kiso A-0975 45	05:19:13.56	-03:24:12.6	12.50			10
VLA 1	05:19:44.02	-05:54:13.2	—			14
VLA 2	05:19:45.36	-05:52:36.6	—			14
VLA 4	05:19:54.77	-05:55:39.4	—			14
VLA 5	05:19:58.92	-05:53:49.9	—			14
Kiso A-0975 86	05:25:39.79	-04:11:02.0	15.50			10
L 1616, L 1615, CB 28:						
IRXS J045912.4-033711	04:59:14.59	-03:37:06.3	11.73	G8		17, 15
IRXS J050416.9-021426	05:04:15.93	-02:14:50.5	12.96	K3		17, 15
UX Ori †	05:04:29.99	-03:47:14.3	9.61	A3e	HBC 430, IRAS 05020-0351, HD 293782	11, 16
TTS 050513.5-034248	05:05:13.47	-03:42:47.8	—	M5.5		17
TTS 050538.9-032626	05:05:38.85	-03:26:26.4	17.30	M3.5		17
RX J0506.6-0337	05:06:34.95	-03:37:15.9	12.23	G7		17, 15

Table 9. Continued

Clouds / Identifier	α (2000) h m s	δ (2000) ° ′ ″	V	Spectral Type	Other identification	Refs.
TTS 050644.4-032913	05:06:44.42	-03:29:12.8	17.69	M4.5		17
TTS 050646.1-031922	05:06:46.05	-03:19:22.4	17.34	K4		17,15
RX J0506.8-0318	05:06:46.64	-03:18:05.6	14.86	K8.5		17,15
TTS 050647.5-031910	05:06:47.45	-03:19:09.7	20.51	M5.5		17
RX J0506.8-0327	05:06:48.32	-03:27:38.2	15.96	M3.5		17,15
RX J0506.8-0305	05:06:48.98	-03:05:42.9	17.33	M4.5		17
TTS 050649.8-031933	05:06:49.77	-03:19:33.1	17.63	M3.5		17
TTS 050649.8-032104	05:06:49.78	-03:21:03.6	18.59	M1		17
TTS 050650.5-032014	05:06:50.50	-03:20:14.3	21.11	M6.5		17
TTS 050650.7-032008	05:06:50.74	-03:20:08.0	19.54	M4.5		17
RX J0506.9-0319 NW	05:06:50.83	-03:19:35.2	16.73	M3		17,15
RX J0506.9-0319 SE	05:06:50.99	-03:19:38.0	14.82	K5	L 1616 MIR5	17,15,18
HD 293815	05:06:51.05	-03:19:59.9	10.08	B9		17,15,19
RX J0506.9-0320W	05:06:52.86	-03:20:53.2	15.33	K8.5	L 1616 MIR2	17,15,18
RX J0506.9-0320E	05:06:53.32	-03:20:52.6	15.74	K1	L 1616 MIR1	17,15,18
TTS 050654.5-032046	05:06:54.53	-03:20:46.0	-	M4		17
LkH α 333 †	05:06:54.65	-03:20:04.8	14.19	K4	HBC 82, RX J0506.9-0320, Kiso A-0974-14	17,15, 20, 11, 43
L 1616 MIR4	05:06:54.93	-03:21:12.7	18.99	K1		17, 13, 12, 18
Kiso A-0974-15	05:06:55.52	-03:21:13.2	12.84	B3		17, 15,18, 21, 20, 22, 23
RX J0507.0-0318	05:06:56.94	-03:18:35.5	15.21	M0	NSV 1832, L 1616 MIR3, IRAS 05044-0325	17,15
TTS 050657.0-031640	05:06:56.97	-03:16:40.4	17.69	M4.5		17
TTS 050704.7-030241	05:07:04.71	-03:02:41.0	20.04	M6		17
TTS 050705.3-030006	05:07:05.32	-03:00:06.2	15.50	M0		17
RX J0507.1-0321	05:07:06.10	-03:21:28.2	16.13	M1	Kiso A-0974-16	17,15,18, 20, 43
TTS 050706.2-031703	05:07:06.22	-03:17:02.9	19.99	M6		17
RX J0507.2-0323	05:07:10.95	-03:23:53.4	13.95	K4	Kiso A-0974-18	17,15,18, 20

Table 9. Continued

Clouds / Identifier	α (2000) h m s	δ (2000) ° ′ ″	V	Spectral Type	Other identification	Refs.
TTS 050713.5–031722	05:07:13.52	–03:17:22.1	17.57	K8.5		17
RX J0507.3–0326	05:07:14.99	–03:26:47.3	14.31	M0		17
TTS 050717.9–032433	05:07:17.85	–03:24:33.1	16.67	M2.5		17, 15
RX J0507.4–0320	05:07:22.28	–03:20:18.5	16.71	M4		17, 15
RX J0507.4–0317 ^a	05:07:25.93	–03:17:12.3	17.19	M3		17
TTS 050729.8–031705	05:07:29.80	–03:17:05.1	20.83	M6.5		17
TTS 050730.9–031846	05:07:30.85	–03:18:45.6	22.12	M5.5		17
TTS 050733.6–032517	05:07:33.58	–03:25:16.7	19.62	M5.5		17
TTS 050734.8–031521	05:07:34.83	–03:15:20.7	19.05	M5		17
RX J0507.6–0318 ^a	05:07:37.67	–03:18:15.6	15.16	K7		17
TTS 050741.0–032253	05:07:41.00	–03:22:53.0	17.55	M4		17
TTS 050741.4–031507	05:07:41.35	–03:15:06.7	17.92	M4.5		17
TTS 050752.0–032003	05:07:51.95	–03:20:02.8	19.55	M5.5		17
TTS 050801.4–032255	05:08:01.43	–03:22:54.5	–	M0.5		17, 15
TTS 050801.9–031732	05:08:01.94	–03:17:31.6	–	M1		17, 15
TTS 050804.0–034052	05:08:04.00	–03:40:51.7	–	M2.5		17, 15
TTS 050836.6–030341	05:08:36.55	–03:03:41.4	–	M1.5		17, 15
TTS 050845.1–031653	05:08:45.10	–03:16:52.5	–	M3.5	Kiso A-0974-21	17, 15
RX J0509.0–0315 [†]	05:09:00.66	–03:15:06.6	11.39	G8	IRXS J050859.6–0315–03	17, 15
RX J0510.1–0427 [†]	05:10:04.60	–04:28:03.7	11.73	K4	IRX J051004.9–042757	17, 15
IRXS J051011.5–025355	05:10:10.86	–02:54:04.9	12.42	K0	V1011 Ori, IRAS 07076-0257	17, 15, 24, 12
RX J0510.3–0330 [†]	05:10:14.78	–03:30:07.4	11.74	G8	IRXS J051015.7-033001	17, 15, 4, 6
IRXS J051043.2–031627	05:10:40.50	–03:16:41.6	11.38	G2		17, 15
RX J0511.7–0348 [†]	05:11:38.93	–03:48:47.1	12.02	K1		17, 15, 4, 6
RX J0512.3–0255 [†]	05:12:20.53	–02:55:52.3	12.61	K2	V531 Ori	17, 15, 4, 12, 24, 6, 43
L 1616 MMS1 A	05:06:44.40	–03:21:34.0	–	–		18
L 1616 MMS1 B	05:06:43.70	–03:21:28.0	–	–		18

Table 9. Continued

Clouds / Identifier	α (2000) h m s	δ (2000) ° ' "	V	Spectral Type	Other identification	Refs.
L 1616 MMS1 C	05:06:43.40	-03:21:38.0	-	-		18
L 1616 MMS1 D	05:06:42.90	-03:21:31.0	-	-		18
IC2118:						
RX J0500.4-1054	05:00:25.83	-10:54:22.3	13.00	K7		6, 4, 5
IRAS 04591-0856	05:01:30.20	-08:52:14.0	-	-	G 13, HHL 17	25, 26
2MASS J05020630-0850467 †	05:02:06.31	-08:50:46.6	-	M2IV		26, 27
RX J0502.4-0744 †	05:02:20.84	-07:44:09.9	11.21	G6		6, 4, 5
RX J0503.8-1130 †	05:03:49.55	-11:31:01.0	-	K1		6, 4, 5
2MASS J05065349-0617123 †	05:06:53.51	-06:17:12.5	-	K7IV	IRAS F 05044-0621	26, 27
2MASS J05071157-0615098 †	05:07:11.57	-06:15:10.0	-	M2IV	IRAS F 05047-0618	26, 27
2MASS J05073016-0610158 †	05:07:30.18	-06:10:15.8	-	K6IV	IRAS 05050-0614, Kiso A-0974 19	26, 27, 10, 43
2MASS J05073060-0610597 †	05:07:30.62	-06:10:59.7	-	K7IV		26, 27, 43
RX J0507.8-0931 †	05:07:48.33	-09:31:43.2	-	K2		6, 4, 5
<i>Candidates in IC 2118:</i>						
2MASS J05060574-0646151	05:06:05.75	-06:46:15.2	-	G8 :		26
2MASS J05094864-0906065	05:09:48.65	-09:06:06.6	-	G8		26
2MASS J05112460-0818320	05:11:24.60	-08:18:32.1	-	M0		26
L 1642:						
BD-15 808 †	04:32:43.51	-15:20:11.3	10.39	G4V	GSC 05891-00069, 1RXS J043243.2-152003	28
L 1642-2 †	04:34:49.73	-14:13:08.1	17.00	-	HBC 410, IRAS 04325-1419	11, 29, 30, 31
L 1642-2B	04:34:49.98	-14:13:12.8	-	-	2MASS J04344997-1413128	29
L 1642-1 †	04:35:02.29	-14:13:40.8	13.70	K7IV	EW Eri, HBC 413, IRAS 04327-1419	11, 29, 30
2MASS J04351455-1414468	04:35:14.55	-14:14:46.9	-	-	2MASS J0435145-141446	32
IRAS 04336-1412	04:35:55.30	-14:05:58.0	-	-	L 1642-3	29, 33
IRAS 04347-1415	04:37:03.40	-14:09:01.0	-	-	L 1642-4	29, 33

Table 9. Continued

Clouds / Identifier	α (2000) h m s	δ (2000) ° ′ ″	V	Spectral Type	Other identification	Refs.
<i>Candidates:</i>						
IRAS 04342-1444	04:36:33.88	-14:38:58.0	9.03	K5	BD-14 929, GSC 05327-00570, HIP 21463	33
IRAS 04349-1436	04:37:13.20	-14:30:34.0				33
LBN 991:						
RX J0513.4-1244 †	05:13:22.02	-12:44:52.4	10.70	G4	GSC 05338-00490	6, 4
LBN 917, LBN 906:						
IRAS 04451-0539	04:47:34.10	-05:34:14.0	14.76		PDS 13	34
Anonymous X-ray clump at						
	$\alpha \approx 5^h 21^m$	$\delta \approx -9^\circ$				
RX J0515.6-0930 †	05:15:36.30	-09:30:51.8	9.79	G5		6, 4
RX J0522.1-0844	05:22:03.40	-08:44:19.0	12.09	K0		6, 4
RX J0523.0-0850 †	05:22:57.00	-08:50:11.5	-	K7-M0		6, 4
IRAS 05222-0844	05:24:37.00	-08:42:00.0	9.88	G3	PDS 111, BD-08 1115, IRXS J052437.4-084200	35
OS98-27, 35, 40, 41: Globules around σ Ori						
YSO CB031YC1	05:30:45.00	-00:38:15.00	14.10	M1		36
CVSO 121	05:33:39.82	-00:38:54.20	14.30	K3		37
YSO CB032YC1	05:36:30.64	-00:18:43.60	14.0:	-		36
IRAS 05355-0146	05:38:04.90	-01:45:09.00	-	-		38
<i>Candidates:</i>						
Kiso A-0904 10	05:33:00.60	-00:36:21.00	13.20	-		40
IRAS 05337-0019	05:36:20.90	-00:17:16.00	10.37	-		42
OriI-2N-1	05:37:51.10	-01:36:17.00	-	-	TYC 4766-2306-1	39
OriI-2N-2	05:37:59.10	-01:36:56.00	-	-		39
OriI-2N-3	05:38:02.40	-01:36:35.00	-	-		39
OriI-2N-4	05:38:02.60	-01:34:40.00	-	-	2MASS J05380259-0134392	39
Kiso A-0976 331	05:38:25.00	-05:22:06.00	16.00	-	Haro 4-107, PACH 468	40, 41

†: proper motion available in Ducourant et al. (2005)

References: **1.** Maheswar, Manoj, & Bhatt (2003); **2.** Downes & Keyes (1988); **3.** Stephenson (1986); **4.** Alcalá et al. (2000); **5.** Alcalá, Chavarría & Terranegra

(1998); **6.** Alcalá et al. (1996); **7.** Hodapp & Ladd (1995); **8.** Davis et al. (1997); **9.** Weaver & Jones (1992); **10.** Wiramihardja et al. (1991); **11.** Herbig & Bell (1988); **12.** Kinnunen & Skiff (2000); **13.** Chavarria et al. (2000); **14.** Beltrán et al. (2002); **15.** Alcalá et al. (2004); **16.** Natta et al. (1999, 2000); **17.** Gandolfi et al. (2008); **18.** Stanke et al. (2002); **19.** Nesterov et al. (1995); **20.** Nakano, Wiramihardja, & Kogure (1995); **21.** Yonekura et al. (1999); **22.** Cohen et al. (1989); **23.** Olnon, Raimond, & Iras Science Team (1986); **24.** Cieslinski, Jablonski, & Steiner (1997); **25.** Gyul'budaghian (1982); Gyul'budaghian et al. (1987); **26.** Kun et al. (2004); **27.** Kun & Nikolic (2003); **28.** Li et al. (2000); **29.** Sandell et al. (1987); **30.** Osterloh & Beckwith (1995); **31.** Magnani et al. (1995); **32.** Cruz et al. (2003); **33.** Lehtinen et al. (2004); **34.** Gregorio-Hetem et al. (1992); **35.** Gregorio-Hetem & Hetem (2002); **36.** Yun et al. (1997); **37.** Briceño et al. (2005); **38.** Mader et al. (1999); **39.** Ogura, Sugitani & Pickles (2002); **40.** Wiramihardja et al. (1989); **41.** Haro (1949); **42.** Magakian (2003); **43.** Lee & Chen (2007) **44.** Seale & Looney (2008)